The phylogeny of Sericini and their position within the Scarabaeidae based on morphological characters (Coleoptera: Scarabaeidae)

D I R K A H R E N S

Deutsches Entomologisches Institut im Zentrum für Agrarlandschafts- und Landnutzungsforschung Müncheberg, Germany

Abstract. To reconstruct the phylogeny of the Sericini and their systematic position among the scarabaeid beetles, cladistic analyses were performed using 107 morphological characters from the adults and larvae of forty-nine extant scarabaeid genera. Taxa represent most 'traditional' subfamilies of coprophagous and phytophagous Scarabaeidae, with emphasis on the Sericini and other melolonthine lineages. Several poorly studied exoskeletal features have been examined, including the elytral base, posterior wing venation, mouth parts, endosternites, coxal articulation, and genitalia. The results of the analysis strongly support the monophyly of the 'orphnine group' + 'melolonthine group' including phytophagous scarabs such as Dynastinae, Hopliinae, Melolonthinae, Rutelinae, and Cetoniinae. This clade was identified as the sister group to the 'dung beetle line' represented by *Aphodius* + *Copris*. The 'melolonthine group' is comprised in the strict consensus tree by two major clades and two minor lineages, with the included taxa of Euchirinae, Rutelinae, and Dynastinae nested together in one of the major clades ('melolonthine group I'). Melolonthini, Cetoniinae, and Rutelinae are strongly supported, whereas Melolonthinae and Pachydemini appear to be paraphyletic. Sericini + Ablaberini were identified to be sister taxa nested within the second major melolonthine clade ('melolonthine group II'). As this clade is distributed primarily in the southern continents, one could assume that Sericini + Ablaberini are derived from a southern lineage. Plausibly, ancestors of Sericini + Ablaberini and *Athlia* were separated by a vicariance event, such as the separation of the African plate from the rest of Gondwana, whereas Sericini and Ablaberini probably diversified during the early Tertiary, with dispersal of some basal Sericini to South America.

Introduction

The family Scarabaeidae (Scholtz, 1990) is one of the more intensively studied groups of beetles with respect to their biology, taxonomy, and phylogeny. However, Sericine chafers, with 4000 described species in about 200 genera,

represent a striking exception, being poorly known in terms of phylogeny, taxonomy, and larval morphology. The tribe Sericini occurs in the Holarctic (apart from the polar and subpolar region), Palaeotropic and Neotropic region, being most diverse in tropical and subtropical zones (Fig. 1). It is absent entirely in New Guinea, Australia, New Zealand, and southern South America.

As with other groups of phytophagous Scarabaeidae, adult Sericini are generalist herbivores. *Maladera castanea* (Arrow, 1913) feeds on more than 100 different plant species, preferring some thirty host plants with succulent roots (Tashiro, 1987). The larvae, known as white grubs, feed on roots and underground stems of living plants (Ritcher,

Correspondence: Dirk Ahrens, Deutsches Entomologisches Institut im Zentrum für Agrarlandschafts- und Landnutzungsforschung Müncheberg, Eberswalder Str. 84, D-15374 Müncheberg, Germany. E-mail: ahrens.dirk_col@gmx.de
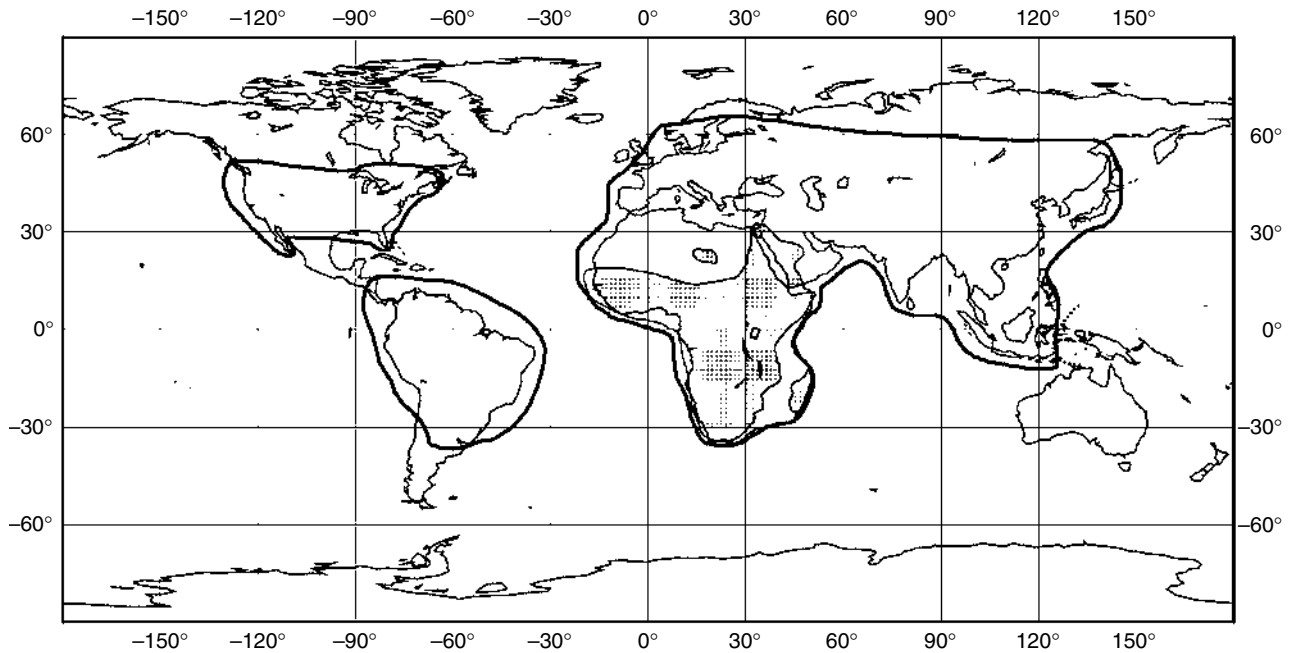
Fig. 1. World-wide distribution of the Sericini (bold line). The Ablaberini (the presumed sister taxon according to Machatschke, 1959 – grey shaded) are limited to the Afrotropical region.

1966). Many species have been reported as crop pests. The life cycle may take 1 or 2 years, depending on the climatic conditions (Horion, 1958; Tashiro, 1987). The average longevity of adults is about 1 month (Tashiro, 1987). In the northern hemisphere, sericines overwinter in the larval stage, mainly as the third instar, by migrating into deeper soil layers. Many species of sericine chafers are nocturnal, and have an inconspicuous dark or brown colour. Sericines often hide underground during the day (Tashiro, 1987). At dusk, the beetles come to the surface and feed on nearby plants. Low temperatures may reduce flight activities significantly (Ahrens, unpublished).

Several hypotheses have been presented for the systematic position of the Sericini, but traditional placement has been with other groups of phytophagous Scarabaeidae in the subfamily Melolonthinae (Dalla Torre, 1912; Browne & Scholtz, 1998). The phylogeny of phytophagous Scarabaeidae has been studied and discussed recently by several authors, but most provide no formal cladistic analysis (Machatschke, 1959; Iablokov-Khnzorian, 1977; Nikolaev, 1998) and those who do consider the Sericini only superficially (Howden, 1982; Zunino & Monteresino, 1990; Scholtz & Chown, 1995; Browne & Scholtz, 1996, 1998, 1999; Jameson, 1998; Sanmartín & Martín-Piera, 2003). Machatschke (1959) hypothesized the monophyly of the subfamily Sericinae containing the tribes Diphucephalini, 'Camentini' (= Ablaberini), and Sericini using the following characters: (a) the labrum and clypeus on one plane, fused, producing a labroclypeus; (b) the labrum establishes the anterior margin of this

'pseudoclypeus'; (c) anterior coxae conically produced; and (d) posterior coxae widened. He also assigned the known genera of Sericini to three subtribes: Phyllotocina, Sericina, and Trochalina. Although Machatschke (1959) based the monophyly of Sericinae on characters that might be considered as 'good' apomorphies, the characters used to argue for the monophyly of Melolonthinae have to be considered in great part unambiguously plesiomorphic, such as the separated labrum and clypeus and the transversal carina of the anterior coxae. The arguments for the monophyly of Sericinae + Melolonthinae are unconvincing because of confusion between apomorphies and plesiomorphies in his argumentation scheme (e.g. position of stigmata within abdominal sternites).

Browne & Scholtz (1998) presented a phylogenetic analysis based on the comparative morphology of articulation and base of the hind wing of Scarabaeidae. They examined numerous genera of sixteen high-ranked scarabaeid taxa traditionally classified as subfamilies, as well as taxa of uncertain phylogenetic status. According to their phylogenetic hypothesis, the Scarabaeidae comprised two major lineages: the 'aphodiine line' (containing Aphodiinae, including Aegialiini, *Aulonocnemis*, and Scarabaeinae), and the 'orphnine line' (containing Orphninae and all major subfamily taxa of phytophagous scarabs). However, their melolonthine lineage comprising the 'Melolonthinae', *Acoma*, *Chaunanthus*, *Oncerus*, and the Hopliini was based on few apomorphies only, in contrast to most other clades. Moreover, they realized that the wing base offered few suitable characters to investigate

the Melolonthinae phylogeny in more detail due to a lack of significant differences.

In contrast to coprophagous Scarabaeidae and 'older' lineages of Scarabaeoidea (Scholtz *et al.*, 1994; Scholtz & Chown, 1995; Scholtz & Browne, 1996; Browne & Scholtz, 1999; Pretorius *et al.*, 2000), the phylogeny of phytophagous Scarabaeidae is far from being resolved (Sanmartín & Martín-Piera, 2003). This is strikingly evident when trying to place known fossils into the present phylogenetic system (Krell, 2000).

Here, a cladistic analysis of morphological characters was performed to determine the phylogenetic position of Sericini and their phylogenetic relationships to other phytophagous lineages of Scarabaeidae. The selected taxa represent most widely recognized subfamilies of coprophagous and phytophagous Scarabaeidae (Nikolaev, 1998), with emphasis on the Sericini and melolonthine lineages.

Materials and methods

Taxon sampling

This study included forty-nine taxa representing twelve subfamilies, twenty-four tribes, and forty-eight genera of Scarabaeidae. Character and character state descriptions were based on the examination of ninety-two species belonging to sixty-six genera (see Appendix 1). For several genera, particularly the larger ones such as *Aphodius*, *Maladera*, or *Serica*, more than one species was scored. For the elaboration of character systems not previously utilized for cladistic analysis, such as structures of mesendosternites or elytral base, many additional genera of Scarabaeoidea have been examined to assess variation within these structures. The material studied for this analysis originated mainly from the author's collection (CA) or from the collection of the Deutsches Entomologisches Institut, Müncheberg (DEI).

The outgroup, *Trox sabulosus* (Trogidae), was chosen based on the phylogenetic hypothesis of the Scarabaeoidea proposed by Browne & Scholtz (1999). The Trogidae were also recognized as an ancestral Scarabaeoidea lineage in other previous studies (e.g. Howden, 1982; Browne & Scholtz, 1996, 1999), and are certainly not part of the Scarabaeidae clade (Browne & Scholtz, 1998). The choice of taxa included within the ingroup was based mainly on present and historical classification of the Sericini (e.g. Lacodaire, 1856; Dalla Torre, 1912) as well as on relationships discussed by previous authors (e.g. Machatschke, 1959; Iablokov-Khnzorian, 1977; Browne & Scholtz, 1998; Nikolaev, 1998; Sanmartín & Martín-Piera, 2003). Consequently, all major lineages of Scarabaeidae that were potentially closely related to Sericini were considered. Additionally, two taxa (*Aphodius* and *Copris*) were included as a test for an adequate outgroup choice, as they represent the well-supported hypothetical sister clade of the

'melolonthine subgroup' plus Orphninae based on the tree of Browne & Scholtz (1998: fig. 2).

Phylogenetic analysis

The 107 morphological characters had a total of 261 states. Inapplicable characters were coded as '–', whereas unknown character states were coded as '?' (Strong & Lipscomb, 1999). All characters were run equally weighted and nonadditive. The parsimony analysis was performed in NONA 2.0 (Goloboff, 1999) using the parsimony ratchet (Nixon, 1999) implemented in NONA and run in WINCLADA version 1.00.08 as a shell program (Nixon, 2002). Two hundred iterations were performed (one tree hold per iteration). The number of characters to be sampled for reweighting during the parsimony ratchet was determined to be ten. All searches were run under the collapsing option 'ambiguous', which collapses every node whose minimum length is 0. State transformations were considered to be apomorphies of a given node only if they were unambiguous (i.e. without arbitrary selection of accelerated or delayed optimization) and if they were shared by all dichotomized most-parsimonious trees. Bremer support (Bremer, 1988, 1994) and parsimony jackknife (Farris *et al.*, 1996) were calculated using NONA to evaluate the trees. The search was set to a Bremer support level of 12, with seven runs (each holding a number of trees from 100 to 500 times multiple of suboptimal tree length augmentation) and a total hold of 8000 trees. The jackknife value was calculated running 100 replications with 100 search steps (mult*N) having one starting tree per replication (random seed 0). Character changes were mapped on the consensus tree using WINCLADA.

Characters and character states

One hundred and seven characters were coded, including 102 characters from the adult stage: head and its appendages (twenty-one), thoracic (three) and abdominal sclerites (four), legs (twenty), elytral base (seven), posterior wing venation (seven), endosternites (seventeen), thoracic musculature (four), male (fourteen) and female genitalia (five). Five characters were coded from immature stages (third instar). Data on larval morphology were taken from Giljarov (1964), Lumaret & Tauzin (1992), Medvedev (1952), Paulian & Lumaret (1982), Klausnitzer & Krell (1996), Ritcher (1966), and McQuillan (1985), and data on thoracic musculature were based mainly on Larsén (1966). The wing venation terminology used herein follows Kukalová-Peck & Lawrence (1993). Of these 107 characters, seventy were binary and thirty-seven multistate, and all were unordered. The character states are illustrated in Figs 2–13.

In describing character states, I have refrained from formulating any hypothesis about their transformation. In particular, coding is not implying whether a state is derived or ancestral. The data matrix is presented in Appendix 2 and as Supplementary material.
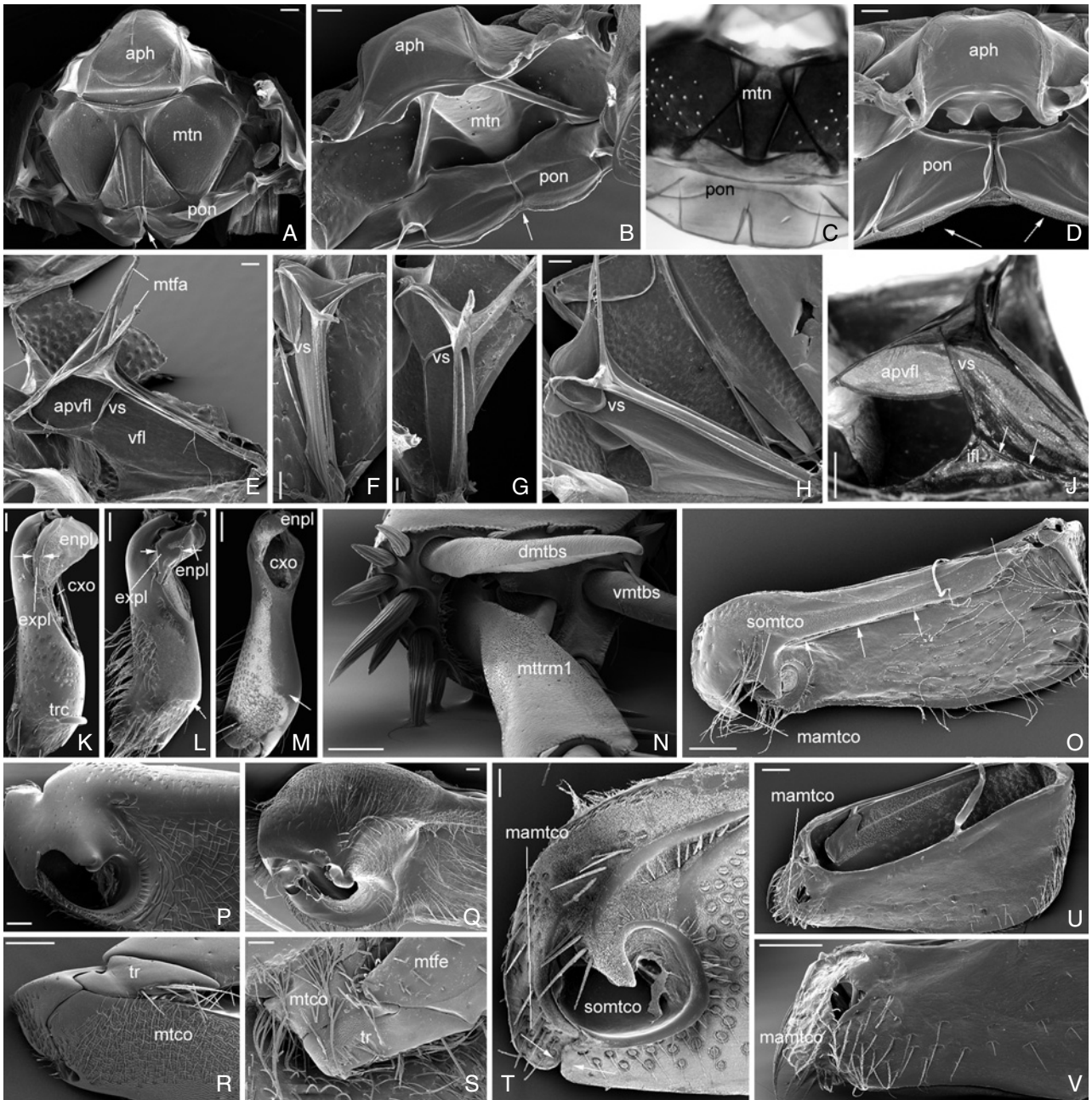
Fig. 2. A, Head, cranial view: *Phyllotocus macleayi*; B, labroclypeus, cranial view: *Calloserica langtangica*; C, maxilla, medioventral view: *Pachypus candidae*; D, galea of maxilla, medioventral view: *Heteronyx* sp.; E, galea of maxilla, mesomedial view: *Paratriodonta romana*; F, maxilla, ventral view: *Diphucephala* sp.; G, galea of maxilla, ventral view: *Hoplia graminicola*; H, lacinia and dorsal process of parastipes (maxilla), medial view: *Sparrmannia* sp.; J, galea of maxilla, mesomedial view: *Orphnus* sp.; K, galea of maxilla, mesomedial view: *Phyllotocus macleayi*; L, maxilla, medial view: *Maladera holosericea*; M, maxilla, medial view: *Cyrtocamenta pygidialis*; N, maxilla, medial view: *Telura alta*; O, galea of maxilla, medial view: *Hymenochelus distinctus*; P, galea of maxilla, ventral view: *Hymenochelus distinctus*; Q, maxilla, medial view: *Chasmatopterus hirtus*; R, maxilla, medial view: *Omaloplia spireae*; S, maxilla, medial view: *Diphucephala* sp.; T, labium, medial view: *Gastroserica marginalis*; U, labium, medial view: *Cyrtocamenta pygidialis*; V, labium, ventrolateral view: *Omaloplia spireae*; W, labium, ventrolateral view: *Pachyserica olafi*. Scale: G, N, O = 30 μm; A–F, H–M, P–W = 100 μm.

Fig. 3. A, Labium, ventrolateral view: *Phyllotocus macleayi*; B, labium, ventrolateral view: *Adoretus* spec.; C, labium, medial view: *Chasmatopterus hirtus*; D, craniolateral portion of the labium, ventral view: *Diphucephala* spec.; E, labium, ventrolateral view: *Trochalus* sp.; F, labium, cranial view: *Pachypus candidae*; G, craniolateral portion of the labium, ventral view: *Sericoides* sp.; H, mesofurca and metafurca, cranial view: *Anaplotrupes stercorosus*; J, mesofurca, cranial view: *Aphodius scutator*; K, mesofurca, craniolateral view: *Hymenoplia castilliana*; L, mesofurca, craniolateral view: *Maladera holosericea*; M, mesofurca, craniolateral view: *Anisoplia segetum*; N, mesofurcal arm, craniolateral view: *Pseudopanotrogus clypealis*; O, mesofurca, craniolateral view: *Protaetia cuprea*; P, mesofurca, lateral view: *Phyllotocus macleayi*; Q, mesofurca, lateral view: *Hymenoplia castilliana*; R, mesofurca, lateral view: *Aphodius scutator*; S, mesofurcal arm, cranial view: *Maladera holosericea*; T, mesofurca, lateral view: *Raysymmela pallipes*; U, mesofurcal arm, cranial view: *Onthophagus* spec.; V, mesonotum, medial view: *Raysymmela pallipes*; W, mesonotum, medial view: *Omaloplia spireae*; X, mesonotum, medial view: *Sericania fuscolineata*. Scale: D, F = 20 µm; A, C, G, M, N, P, Q, S–V = 100 µm; B, E, J, K, L, R = 200 µm; O = 300 µm; W, X = 500 µm; H = 1 mm.

Fig. 4. A, Metanotum, medial view: *Pseudopanotrogus clypealis*; B, metanotum, cranial view: *Hymenoplia castilliana*; C, metanotum, medial view: *Chasmatopterus hirtus*; D, metanotum, cranial view: *Athlia rustica*; E, metafurca, lateral view: *Chasmatopterus hirtus*; F, metafurca, lateral view: *Phyllotocus macleayi*; G, metafurca, lateral view: *Camenta westermanni*; H, metafurca, lateral view: *Maladera holosericea*; J, metafurca, lateral view: *Propomacrus mucronatus*; K, procoxa, cranial view: *Panotrogus nepalensis*; L, procoxa, cranial view: *Hymenoplia castilliana*; M, procoxa, medial view: *Maladera holosericea*; N, metatibia, apical view: *Pleophylla* sp.; O, metacoxa, ventral view: *Chasmatopterus hirtus*; P, metacoxa apical portion, ventral view: *Protaetia cuprea*; Q, metacoxa apical portion, ventral view: *Geotrupes stercorosus*; R, metacoxa apical portion, caudoventral view: *Onthophagus fracticornis*; S, metacoxa apical portion, ventral view: *Diphucephala* sp.; T, metacoxa apical portion, ventral view: *Maladera holosericea*; U, metacoxa, medial view: *Hymenoplia castilliana*; V, metacoxa, caudal view: *Hymenoplia castilliana*. Scale: B, E, J, N, S, T = 100 μm; D, F–H, K, L, O, Q, R, U, V = 200 μm; A, M, P = 300 μm.
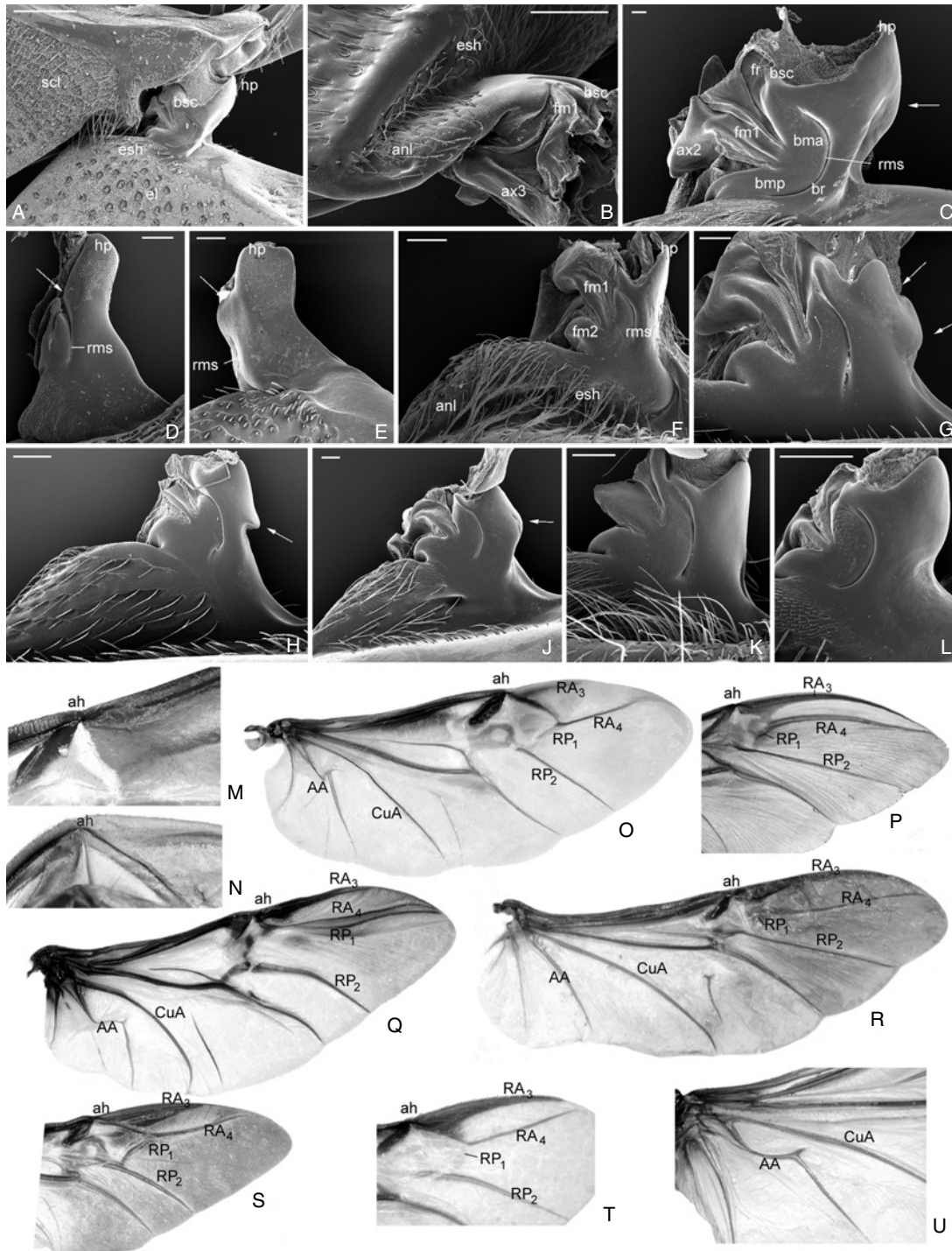
Fig. 5. A, Elytral–scutellar articulation, dorsal view: *Maladera holosericea*; B, elytral basis, mesodorsal view: *Adoretus* sp.; C, elytral basis, dorsal view: *Maladera holosericea*; D, elytral basis, dorsal view: *Valgus hemipterus*; E, elytral basis, dorsal view: *Protaetia cuprea*; F, elytral basis, dorsal view: *Pachypus candidae*; G, elytral basis, dorsal view: *Camenta westermanni*; H, elytral basis, dorsal view: *Orphnus* sp.; J, elytral basis, dorsal view: *Raysymmela pallipes*; K, elytral basis, dorsal view: *Melolontha melolontha*; L, elytral basis, dorsal view: *Hymenoplia castilliana*; M, ala, cranial margin, dorsal view: *Osmoderma eremita*; N, ala, cranial margin, dorsal view: *Camenta westermanni*; O, ala, dorsal view: *Maladera simlana*; P, ala, apical portion, dorsal view: *Propomacrus mucronatus*; Q, ala, dorsal view: *Aphodius scutator*; R, ala, dorsal view: *Tropinota hirta*; S, ala, apical portion, dorsal view: *Hoplia graminicola*; T, ala, apical portion, dorsal view: *Acoma* sp.; U, ala, basal portion, dorsal view: *Propomacrus mucronatus*. Scale: C = 20 μm; J = 30 μm; D, G, H, L = 100 μm; A, B, E, F, K = 200 μm; M–U not to scale.
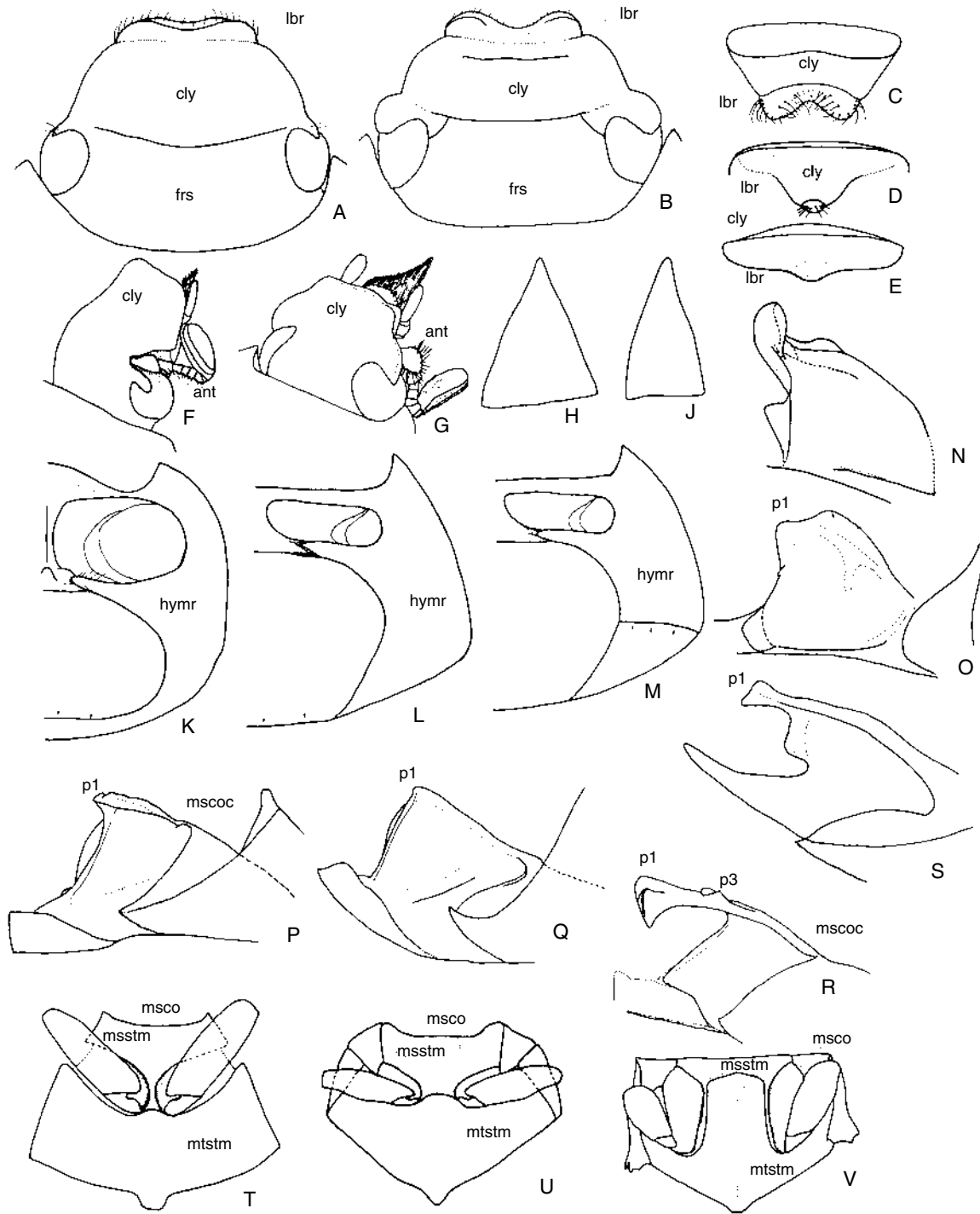
Fig. 6. A, Head, dorsal view: *Athlia rustica*; B, head, dorsal view: *Camenta westermanni*; C, labrum, cranial view: *Melolontha melolontha*; D, labrum, cranial view: *Europteron gracile*; E, labrum, cranial view: *Pachypus candidae*; F, head, dorsolateral view: *Protaetia cuprea*; G, head, dorsolateral view: *Propomacrus mucronatus*; H, stipes (maxilla), ventral view: *Melolontha melolontha*; J, stipes (maxilla), ventral view: *Maladera holosericea*; K, prothorax, ventral view: *Europteron gracile*; L, prothorax, ventral view: *Hyposerica* sp.; M, prothorax, ventral view: *Maladera simlana*; N, mesofurca, lateral view: *Protaetia cuprea*; O, mesofurca, lateral view: *Oryctes nasicornis*; P, mesofurca, lateral view: *Orphnus* sp.; Q, mesofurca, lateral view: *Pachypus candidae*; R, mesofurca, lateral view: *Aphodius scrutator*; S, mesofurca, lateral view: *Melolontha melolontha*; T, pterothorax, ventral view: *Adoretus* sp.; U, pterothorax, ventral view: *Maladera renardi*; V, pterothorax, ventral view: *Copris lunaris*. Not to scale.
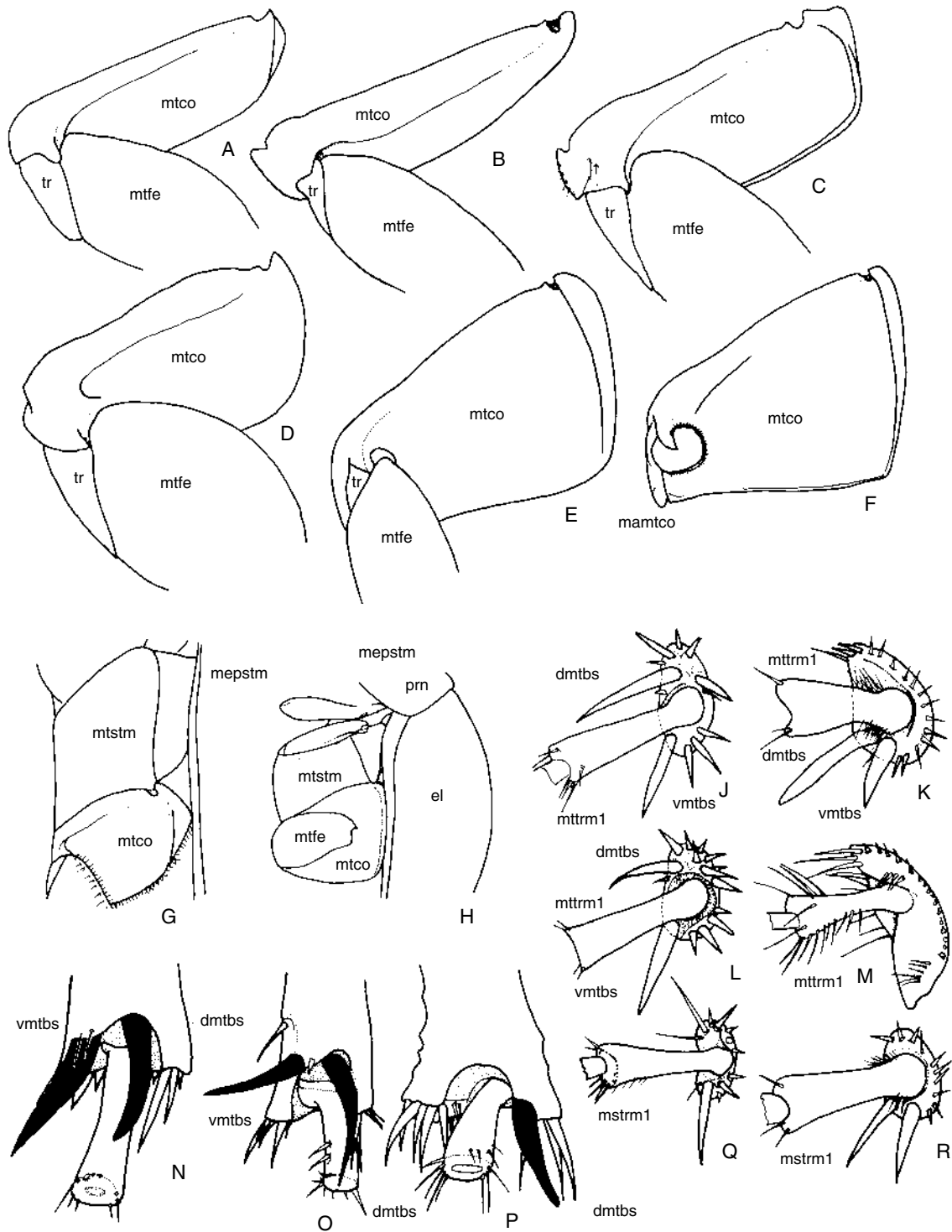
Fig. 7. A, Metacoxa, ventral view: *Aphodius scrutator*; B, metacoxa, ventral view: *Catharsius molossus*; C, metacoxa, ventral view: *Propomacrus mucronatus*; D, metacoxa, ventral view: *Pachypus candidae*; E, metacoxa, ventral view: *Trochalus* sp.; F, metacoxa, ventral view: *Hyposerica* sp.; G, metasternum, lateral view: *Oryctes nasicornis*; H, metasternum, lateral view: *Maladera* sp.; J, metatibia, apical view: *Maladera renardi*; K, metatibia, apical view: *Melolontha melolontha*; L, metatibia, apical view: *Pleophylla* sp.; M, metatibia, apical view: *Diphucephala* sp.; N, metatibia, medial view: *Sericoides* sp.; O, metatibia, medial view: *Phyllotocus macleayi*; P, metatibia, medial view: *Diphucephala* sp., female; Q, mesotibia, apical view: *Maladera renardi*; R, mesotibia, apical view: *Melolontha melolontha*. Not to scale.
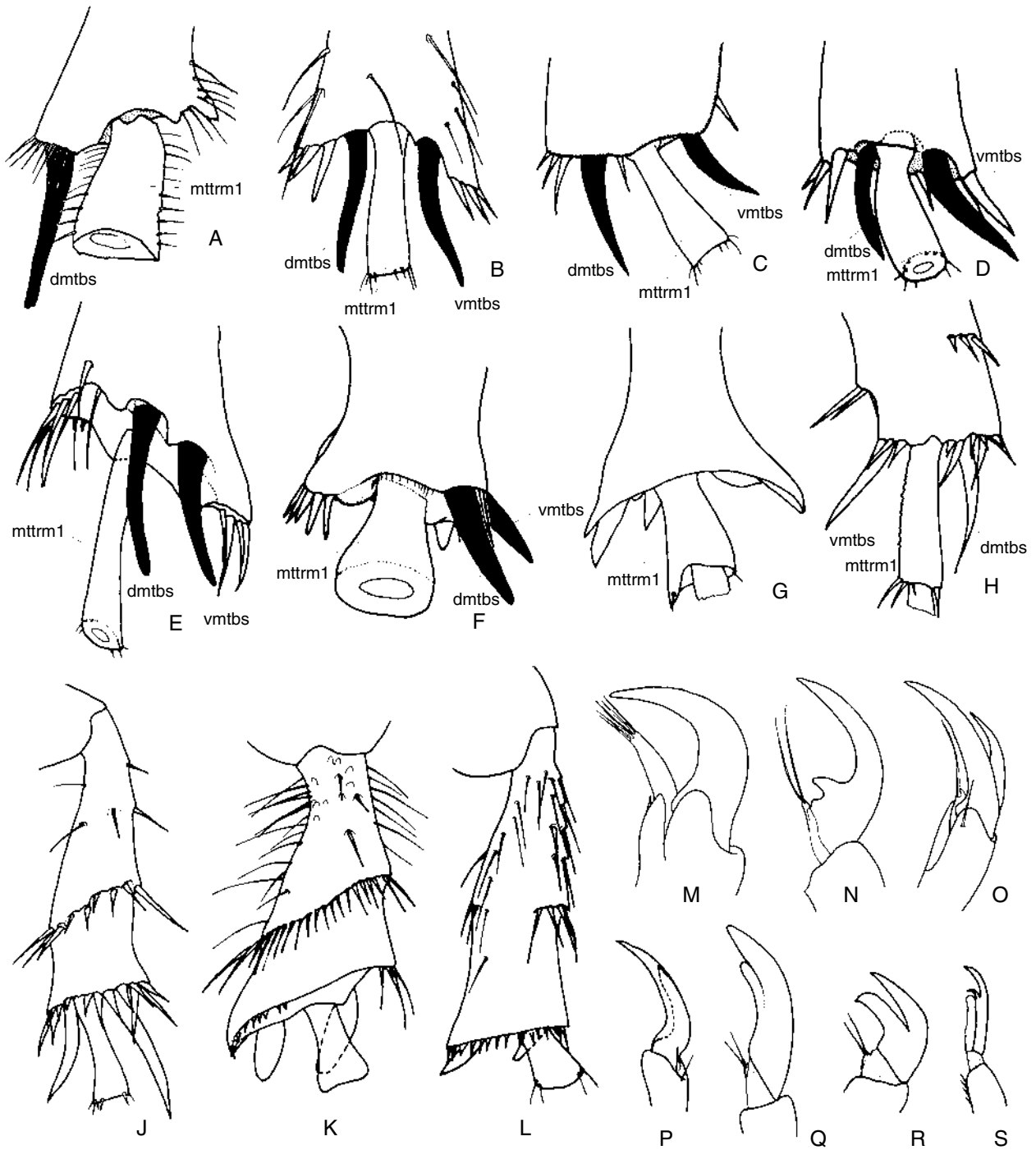
Fig. 8. A, Apical portion of metatibia, medial view: *Catharsius molossus*; B, apical portion of metatibia, medial view: *Empecamenta buettikeri*; C, apical portion of metatibia, medial view: *Maladera insanabilis*; D, apical portion of metatibia, medial view: *Heteronyx* sp.; E, apical portion of metatibia, medial view: *Elaphocera* sp.; F, apical portion of metatibia, medial view: *Anisoplia segetum*; G, apical portion of metatibia, lateral view: *Propomacrus mucronatus*; H, apical portion of metatibia, lateral view: *Maladera insanabilis*; J, metatibia, lateral view: *Hybalus graecus*; K, metatibia, lateral view: *Pachypus candidae*; L, metatibia, lateral view: *Chasmatopterus hirtus*; M, metatarsal claw, lateral view: *Oryctes boas*; N, metatarsal claw, lateral view: *Melolontha melolontha*; O, metatarsal claw, lateral view: *Anisoplia segetum*; P, metatarsal claw, lateral view: *Hoplia graminicola*; Q, metatarsal claw, lateral view: *Cyrtocamenta pygidialis*; R, metatarsal claw, lateral view: *Maladera insanabilis*; S, metatarsal claw, lateral view: *Hymenochelus distinctus*. Not to scale.
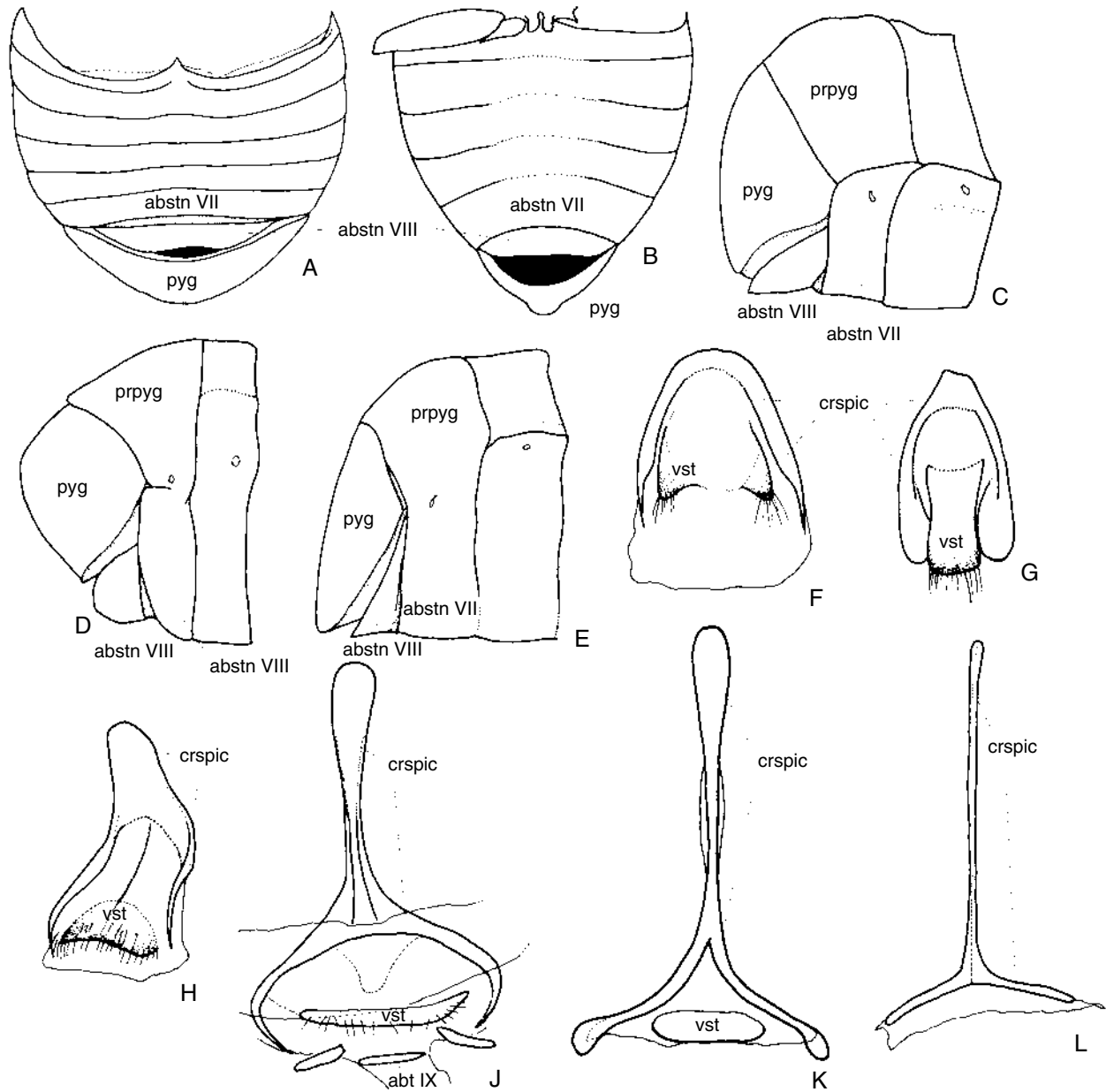
Fig. 9. A, Abdomen, ventral view: *Oryctes nasicornis*; B, abdomen, ventral view: *Melolontha melolontha*; C, abdomen, lateral view: *Nepaloserica procera rufescens*; D, abdomen, lateral view: *Oryctes nasicornis*; E, abdomen, lateral view: *Amphimallon solstitiale*; F, spiculum gastrale, ventral view: *Orphnus* sp.; G, spiculum gastrale, ventral view: *Hybalus graecus*; H, spiculum gastrale, ventral view: *Hoplia graminicola*; J, spiculum gastrale, ventral view: *Athlia rustica*; K, spiculum gastrale, ventral view: *Amphimallon solstitiale*; L, spiculum gastrale, ventral view: *Omaloplia ruricola*. Not to scale.

Adult

Head

1. *Clypeus and labrum*: (0) separated by a suture (Figs 2A, 6A, C, D); (1) fused (Figs 2B, 6B) (CI: 0.50, RI: 0.94).

In the ground pattern of Coleoptera and of Scarabaeoidea, the clypeus and labrum are separated (Matsuda, 1965). Both are fused in *Pachypus*, Ablaberini, Sericini, and *Diphucephala*. Although the labrum is strongly reduced in size in *Pachypus* (Fig. 6E), *Diphucephala* is characterized by a distinct sexual dimorphism affecting the labrum and its fusion with the clypeus where the labrum of the female is usually separated by a distinct suture whereas the separating suture may be completely reduced in the male.

Fig. 10. A–D, Abdominal sternites. A, D, Ventral view; B, C, medial view. A, *Chasmatopterus hirtus*; C, *Athlia rustica*; D, *Cyrtocamenta pygidialis*. E, Spiculum gastrale: *Camenta westermanni*; F, G, K, aedeagus, ventral view; H, apex aedeagus, lateral view; F, H, *Paratriodonta romana*; J, apex aedeagus, lateral view; G, J, *Serica pommeranzi*; B, K, *Amiserica chiangdaoensis*; L, aedeagus, ventrolateral view: *Comaserica bergrothi*; M, phallobase, ventrolateral view: *Raysymmela pallipes*; N, phallobase, lateral view: *Hymenoplia castilliana*; O, P, aedeagus, lateral view; O, *Triodontella* sp., P, *Nepaloserica schmidti*. Not to scale.

2. *Lateral margin of clypeus and labrum*: (0) discontinuous (Fig. 6A, B, C); (1) continuous (Fig. 2A, B) (consistency index (CI): 0.33, retention index (RI): 0.88).
3. *Clypeus anterior of eyes*: (0) not deeply sinuate (Figs 2A, 6A, B, G); (1) deeply sinuate (Fig. 6F) (CI: 1.0, RI: 1.0).
4. *Labrum*: (0) subequal in size to clypeus (Figs 2A, B, 6A–C); (1) distinctly smaller than clypeus (Fig. 6D, E) (CI: 1.0, RI: 1.0).

The morphology of the labrum varies considerably among Scarabaeoidea (Nel & de Villiers, 1988; Nel & Scholtz, 1990), soft tissue feeders such as Aphodiinae and Scarabaeinae and others such as Cetoniinae have a moveable membranous labrum covered dorsally by the clypeus. All these taxa are considered to have character state 0.

5. *Number of antennomeres*: (0) nine or ten; (1) eight (CI: 0.14, RI: 0.14).

Krell (1992) discussed the antennal morphogenesis and the teratological fusion of antennomeres within Scarabaeidae, thus evaluating the practicability of the number of antennomeres as a character for phylogenetic systematics. Due to an evolutionary trend of antennomere fusion, the homoplasy of the character is expected to be high. In species of several sericine genera, the number of antennomeres can be either nine or ten. To remove this 'noise' from the cladistic analysis, antenna with nine or ten antennomeres were coded as one character state (0).

6. *Number of teeth of galea*: (0) six; (1) seven; (2) eight (Fig. 2E); (3) without any teeth (Fig. 2C, J, K); (4) five (Fig. 2D, F) (CI: 0.44, RI: 0.80).
7. *Galea*: (0) with a distal movable tooth separated from the galea by a thin membrane (Fig. 2F); (1) all teeth
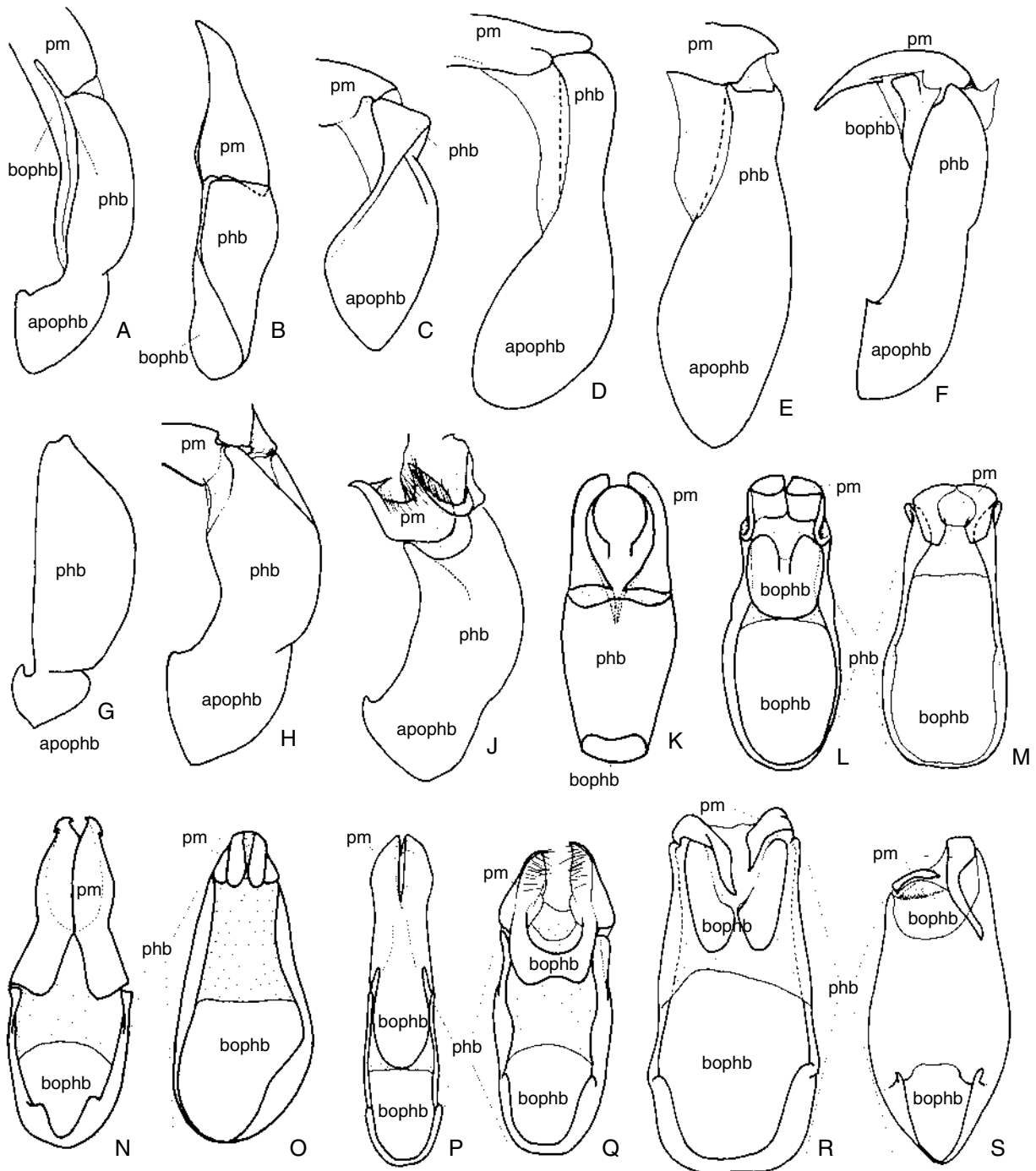
Fig. 11. A, Phallobasis, lateral view: *Adoretus* sp.; B, phallobasis, lateral view: *Aphodius* sp.; C, phallobasis, lateral view: *Chasmatopterus hirtus*; D, phallobasis, lateral view: *Elaphocera tangerina*; E, phallobasis, lateral view: *Athlia rustica*; F, phallobasis, lateral view: *Camenta westermanni*; G, phallobasis, lateral view: *Triodontella* sp.; H, phallobasis, lateral view: *Pleophylla* sp.; J, phallobasis, lateral view: *Omaloplia ruricola*.; K, aedoeagus, ventral view: *Trox sabulosus*; L, aedoeagus, ventral view: *Hybalus graecus*; M, aedoeagus, ventral view: *Phyllotocus macleayi*; N, aedoeagus, ventral view: *Melolontha melolontha*; O, aedoeagus, ventral view: *Elaphocera tangerina*; P, aedoeagus, ventral view: *Adoretus* sp.; Q, aedoeagus, ventral view: *Raysymmela pallipes*; R, aedoeagus, ventral view: *Camenta westermanni*; S, aedoeagus, ventral view: *Serica thibetana*. Not to scale.
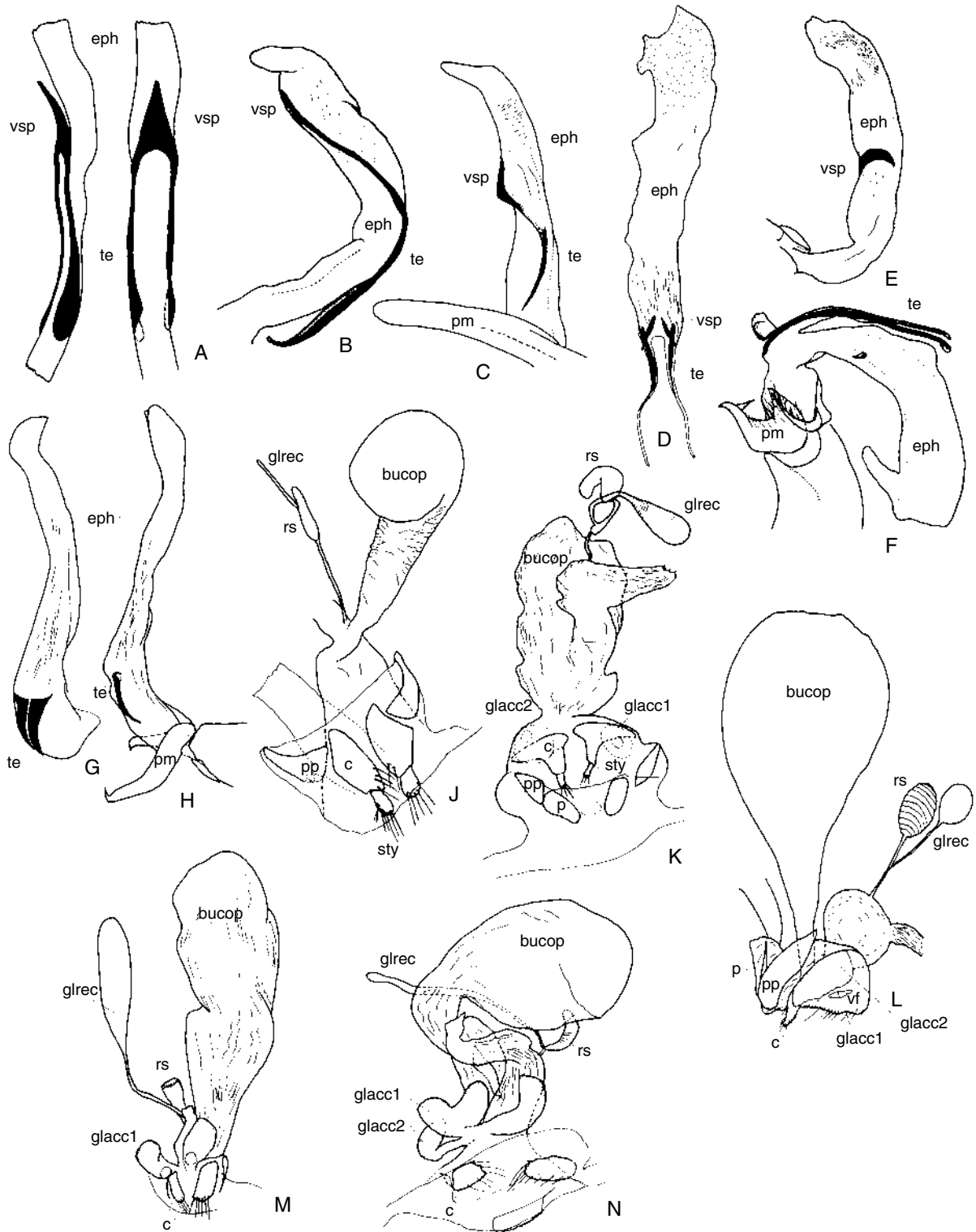
Fig. 12. A, Endophallus, lateral and ventral views: *Aphodius* sp.; B, endophallus, lateral view: *Melolontha melolontha*; C, endophallus, lateral view: *Hoplia graminicola*; D, endophallus, ventral view: *Elaphocera* sp.; E, endophallus, lateral view: *Athlia rustica*; F, endophallus, lateral view: *Omaloplia ruricola*; G, endophallus, ventral view: *Maladera insanabilis*; H, endophallus, lateral view: *Maladera insanabilis*; J, female external genitalia, ventral view: *Trox sabulosus*; K, female external genitalia, ventral view: *Orphnus* sp.; L, female external genitalia, lateral view: *Elaphocera capdeboni*; M, female external genitalia, ventral view: *Phyllotocus macleayi*; N, female external genitalia, ventral view: *Maladera holosericea*. Not to scale.
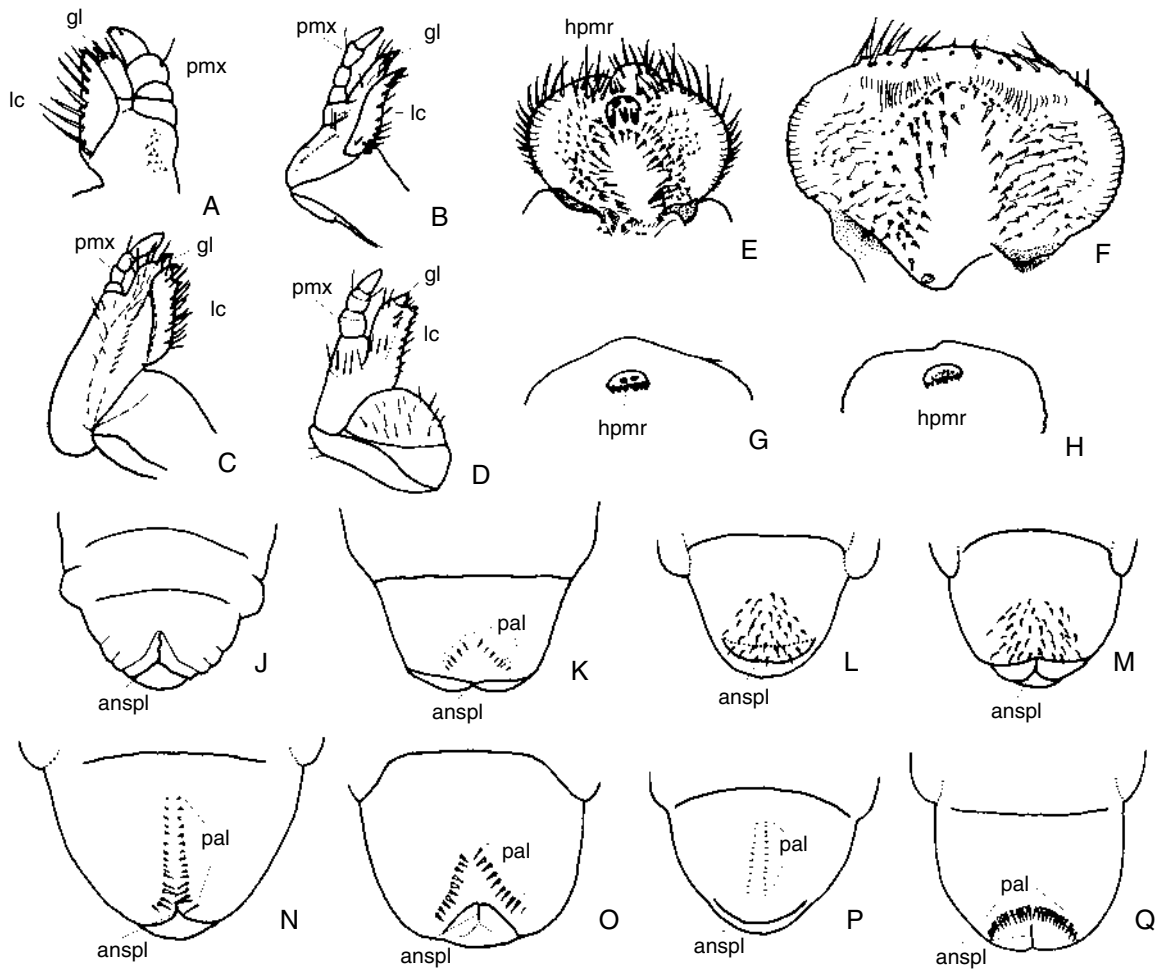
Fig. 13. A, Maxilla, dorsal view: *Trox scaber*; B, maxilla, dorsal view: *Aphodius hamatus*; C, maxilla, dorsal view: *Maladera castanea*; D, maxilla, dorsal view: *Cetonia aurata*; E, epipharynx, ventral view: *Serica ligulata*; F, epipharynx, ventral view: *Propomacrus mucronatus*; G, haptomerum (epipharynx), ventral view: *Heteronyx* sp.; H, haptomerum (epipharynx), ventral view: *Adoretus sinicus*; J, larva, raster: *Trox unistriatus*; K, larva, raster: *Aphodius pardalis*; L, larva, raster: *Adoretus sinicus*; M, larva, raster: *Hoplia equina*; N, larva, raster: *Amphimallon majalis*; O, larva, raster: *Heteronyx* sp.; P, larva, raster: *Anomala orientalis*; Q, larva, raster: *Maladera castanea*. Not to scale.

completely fused with the galea (Fig. 2D); (2) with two separate toothlike spines (Fig. 2G); (3) without teeth, finely setose (Fig. 2K); (4) without teeth, very robustly and finely setose (Fig. 2J); (5) with a distal, movable tooth separated from the galea by an incomplete suture (CI: 0.62, RI: 0.83).

It seems reasonable to discuss whether the distal movable tooth of the galea is homologous with the distogalea. However, the larvae of the taxa in question (*Diphucephala*, *Sericoides*, *Telura*) have a galea with only one joint, consequently this homology seems to be rather improbable. Because the distogalea in Coleoptera does not possess musculature, it is difficult to prove this argument by examination of the maxillary musculature. Character state 2 is only known from Hopliinae (*Hoplia*) and *Phaenomeris*.

8. *Dorsal process of mediostipes, apically*: (0) not widened (Fig. 2L, N, R, S); (1) widened (Fig. 2M); (2) absent

(Fig. 2Q); (3) enlarged and widely fused with lacinia and mediostipes (Fig. 2H) (CI: 0.37, RI: 0.73).

The terminology of the relevant maxillary sclerites is based on Williams (1938) and Beutel (1994). Nel & Scholtz (1990) used the term parastipes for this sclerite, whereas they used 'latero-stipes' for the palpifer, being misled by the strongly developed basal palpifer in Scarabaeidae (see Fig. 2L, M).

9. *Galea*: (0) with basal and distal joint (Fig. 2J); (1) with one joint only (Fig. 2G, H, K) (CI: 1.0, RI: 1.0).
10. *Number of teeth on galea* (visible in ventral view): (0) four; (1) three (CI: 0.20, RI: 0.69).
11. *Dorsal and ventral row of galeal teeth*: (0) on the same level (Fig. 2E, M, N, R); (1) dorsal row basally, ventral row distally displaced (Fig. 2J) (CI: 1.0, RI: 1.0).
12. *Lacinia distally*: (0) long, reaching the teeth of galea, but not fused with galea basally (Fig. 2N); (1) short,

reaching at most the base of the galea (Fig. 2L, M); (2) long, reaching the teeth of the galea, fused with galea basally (Fig. 2Q) (CI: 0.28, RI: 0.50).

The lacinia in Adephaga and in most Polyphaga (including ancestral Scarabaeoidea) is long (e.g. Nel & Scholtz, 1990; Beutel, 1997; Hansen, 1997). This might be evidence to assume that the distally shortened lacinia is a derived character state.

13. *Lacinia basally*: (0) not shortened (Fig. 2L–N); (1) shortened (Fig. 2Q–S); (2) lacinia absent (Fig. 2C) (CI: 0.40, RI: 0.40).
14. *Stipes*: (0) almost twice as long as wide (Fig. 6J); (1) stout, at most a little longer than wide (Fig. 6H) (CI: 0.33, RI: 0.50).
15. *Mentum*: (0) wider than ligular lobes combined (Fig. 2T); (1) as wide as ligular lobes combined or narrower (Fig. 2S, U, V) (CI: 0.10, RI: 0.60).

The terminology of labial appendages suffers from ambiguous homology assessments. Although the mentum was interpreted by Snodgrass (1932, 1935) and Anderson (1936) as a very small basal division of the prementum, workers since Das (1937) have correctly interpreted the larger basal portion (Fig. 2U) as the mentum (Matsuda, 1965). Most authors apply the term ligula for medially fused paraglossal lobes (e.g. Snodgrass, 1932, 1935) or as a collective term for all labial lobes (e.g. Snodgrass, 1935). Assuming that the median fusion of paraglossae evolved more than once in Coleoptera, the term 'ligula', in the first case, might consequently describe nonhomologous structures. The labium of many scarabaeid larvae do not show either glossae or paraglossae, instead they often have a simple ligula (Ritcher, 1966). Ligular muscles, such as the flexor muscle of the glossa or the flexor muscle of the paraglossa in *Periplaneta* (Dorsey, 1943), are not present in Coleoptera (Matsuda, 1965). Nel & Scholtz (1990) used the term 'ligular lobes' (inner/outer) of Snodgrass (1935) to describe the lobe-shaped appendages of the prementum without assessing homology. However, the presence of very small 'glossae' in the quadrilobed ligular type (present in some Scarabaeinae) does not contradict the hypothesis (Crampton, 1928) that in Coleoptera the widely distributed bilobed ligular type (see Williams, 1938) is composed of more or less completely fused paraglossae. Consequently, I assume homology of the ligular lobes in the bilobed ligular type within Scarabaeidae. A stronger sclerotization of the linking membrane between the prementum and the ligular lobes might produce a similar 'ligula'-like median structure, without reduction of lateral ligular lobes or involvement of any portion of the glossa.

16. *Palpiger and prementum*: (0) separated by a suture (Figs 2V, 3G); (1) fused (without a visible suture) (Figs 2W, 3B, E, F); (2) widely separated by a membrane (Fig. 3A) (CI: 0.14, RI: 0.73).
17. *Palpiger and ligular lobes*: (0) separated (Figs 2W, 3A, D, E, G); (1) fused (without a visible suture) (Figs 2V, 3B, F) (CI: 0.14, RI: 0.73).
18. *Palpiger*: (0) not enclosed by prementum and ligular lobe (Fig. 3A); (1) enclosed by prementum and ligular lobe (Fig. 3B, D–G) (CI: 0.50, RI: 0.75).
19. *Palpiger or its homologous equivalent (in ventral view)*: (0) visible (Figs 2V, W, 3A, B, D, E, G); (1) not visible (Figs 2T, U, 3D, F) (CI: 0.09, RI: 0.28).
20. *Prementum and ligular lobe*: (0) separated by a suture (Figs 2V, W, 3A, D, E); (1) fused (without visible suture) (Fig. 3B, F, G) (CI: 0.14, RI: 0.72).
21. *Ligular lobes*: (0) separated (at least by a suture) (Figs 2V, 3A, C–E); (1) fused with each other (Figs 2W, 3B); (2) fused but strongly reduced in size to a small median ligular lobe (Fig. 3F) (CI: 0.25, RI: 0.68).

Thorax

22. *Hypomeron (prothorax) basiventrally*: (0) without transverse carina (Fig. 6K, L); (1) with transverse carina (Fig. 6M) (CI: 0.50, RI: 0.50).

The pronotum of Coleoptera is large and it extends to the ventral surface of the prothorax (Crampton, 1926; Beutel & Haas, 2000). Derivation of the ventral prothoracic portion has long been debated (Matsuda, 1970). Although Ritcher (1969) stated that 'the true origin of the epimeron as a pleural element is indicated in the posterior procoxal bridges of Scarabaeoidea by the lack of any fusion of the epimeron with the prosternum', the currently accepted hypothesis is that, at least for Polyphaga, the propleuron is reduced in length and width (Hlavac, 1975) and that it is internalized and fused with the trochantinus (Beutel, 1997; Beutel & Haas, 2000).

23. *Edge of intersegmental membrane at the basis of pronotum medially (ventral view)*: (0) present and elevated (Fig. 6K); (1) absent (Fig. 6L, M) (CI: 0.50, RI: 0.88).
24. *Pronotum, basal marginal line*: (0) present; (1) absent (CI: 0.10, RI: 0.18).

Although this character is rather variable in many scarab groups, it is apparently very informative among Sericini and is used to obtain a higher resolution of the more derived nodes of the cladogram.

25. *Mesofurcal arm, anterior lamina*: (0) as long as dorsal lamina (Fig. 6Q); (1) shorter than dorsal lamina (Fig. 6N, S); (2) longer than dorsal lamina (Fig. 6P, R) (CI: 0.50, RI: 0.33).
26. *Mesofurcal arm, interior process (p3)*: (0) small (Fig. 3J, T); (1) large (Fig. 3K, L) (CI: 1.0, RI: 1.0).
27. *Mesofurcal arms*: (0) joined by a median sclerotized bridge (Fig. 3J, T); (1) separate, without median bridge (Fig. 3K, L) (CI: 0.20, RI: 0.73).
28. *Mesofurca and mesosternum, carina from craniolateral margin of mesosternum to mesofurcal arm*: (0) absent (Fig. 3H, J, K, T); (1) present (Fig. 3L, S) (CI: 1.0, RI: 1.0).
29. *Mesofurcal arm, craniomedial surface*: (0) large and convex (Fig. 3H, J, K, O, P, T); (1) small and conical (Fig. 3K, L, N); (2) narrow and long (Fig. 3U) (CI: 0.50, RI: 0.83).
30. *Mesofurcal arm, dorsal lamina*: (0) without fringe (Figs 3H–U, 6O–S); (1) with a membranous fringe (Fig. 6N) (CI: 1.0, RI: 1.0).
31. *Mesofurcal arm, dorsal process (p1) compared with the mesocoxal cavity*: (0) very long (as large as the diameter of the coxal cavity) and reflexed (Figs 3J, U, 6R); (1) short (one half to one quarter of diameter of coxal

cavity) and straight (Figs 3K–P, Q, T, 6N, S); (2) very short (less than one eighth of the diameter of the coxal cavity) (Fig. 6O–Q) (CI: 0.33, RI: 0.33).

32. *Mesofurcal arm, dorsal process (p1) apically*: (0) widened (Figs 3H, J, R, 6N, R); (1) narrowed (Figs 3K–P, Q, T, 6N, S); (2) medially widened, in apical portion laterally produced, with acute apex (Fig. 3U) (CI: 0.50, RI: 0.33).

33. *Mesofurcal arm, anterior process (p2)*: (0) present (Fig. 3H, J, M, O, P, T, U); (1) absent (Fig. 3K, L, N, S) (CI: 0.33, RI: 0.83).

34. *Mesofurcal arm, interior process (p3)*: (0) shape lobi-form (Fig. 3K–N, S); (1) shape fringelike (Fig. 3O, U); (2) absent (Fig. 3P) (CI: 0.22, RI: 0.74).

35. *Mesofurcal arm, anterior process (p2)*: (0) separated from anterior lamina (Fig. 3J, M); (1) fused with anterior lamina of mesofurca (Fig. 3N) (CI: 0.50, RI: 0.66).

36. *Median keel of mesonotum (medial view)*: (0) present (Fig. 3V, W); (1) absent (Fig. 3X) (CI: 0.16, RI: 0.58).

37. *Caudal lobes of postnotum (metathorax)*: (0) long and narrow (Fig. 4A); (1) short and wide (Fig. 4B, C); (2) reduced (Fig. 4D) (CI: 0.50, RI: 0.90).

38. *Incision between caudal lobes of postnotum (metathorax)*: (0) deep (Fig. 4A); (1) small or absent (Fig. 4B–D) (CI: 0.25, RI: 0.85).

39. *Anterior and posterior margin of ventral median flange of metendosternite (lateral view)*: (0) convergent towards base or subparallel (Fig. 4F, G); (1) evenly divergent towards base (Fig. 4E, H); (2) extremely divergent in basal half (Fig. 4J) (CI: 0.33, RI: 0.85).

The terminology of the metendosternite is based on Crowson (1944), with reference to de Castro (2001). The strongly divergent anterior and posterior margin of the ventral median flange of the metendosternite is supported by the interiorly strongly produced internal flange of the metasternal longitudinal suture, which closely attaches to the ventral median flange. Both flanges may be completely or partly fused (with a visible suture, Fig. 4J, arrows).

40. *Metafurca, apical portion of ventral median flange (portion apical of ventral suture, lateral view)*: (0) short (shorter than the furcal arm) (Fig. 4F–H); (1) long (as long as the furcal arm, or longer) (Fig. 4E, J) (CI: 0.33, RI: 0.85).

Pretorius *et al.* (2000) noticed that in Scarabaeinae the size of the ventral median flange is reduced in flightless taxa. However, it may also be short in several well-flying groups.

41. *Metafurca, apex of ventral median flange (portion apical of ventral suture, lateral view)*: (0) rounded (Fig. 4F–H); (1) acutely pointed (Fig. 4E, J) (CI: 0.25, RI: 0.78).

Musculature of thorax (nomenclature according to Larsén, 1966). The thoracic musculature of Scarabaeoidea has been studied in some detail by Larsén (1966). For a number of taxa, I was able to examine the thoracic musculature. However, this was not possible for all taxa included in the analysis due to the lack of suitable material. Nevertheless, these characters are important in order to interpret functional relationships to skeletal characters and to reconstruct the ground plan of principal phytophagous scarab lineages.

42. *M37 (M. furco-pleuralis)*: (0) present; (1) absent (CI: 1.0, RI: 1.0).

43. *M49 (M. epimero-trochanteralis)*: (0) present; (1) absent (CI: 1.0, RI: 1.0).

44. *M52 (M. furca-trochanteralis)*: (0) present; (1) absent (CI: 1.0, RI: 1.0).

45. *M78 (M. coxa-basalaris)*: (0) present; (1) absent (CI: 1.0, RI: 1.0).

Legs

46. *Ratio of length of metepisternum/metacoxa*: (0) greater than or equal to 1.0 (Fig. 7G); (1) smaller than 1.0 (Fig. 7H) (CI: 0.50, RI: 0.92).

47. *Ostium of procoxa*: (0) large (at least half as long as the procoxal length) (Fig. 4K, L); (1) small (distinctly less than half as long as procoxal length) (Fig. 4M) (CI: 1.0, RI: 1.0).

48. *Procoxa, transversal carina*: (0) present (Fig. 4K); (1) absent (Fig. 4L, M) (CI: 0.20, RI: 0.71).

The transversal carina and a furrow in the prosternum form a secondary coxo-sternal articulation that fixes the coxa more firmly in its longitudinal rotational axis.

49. *Fusion of the proexopleura and trochantin*: (0) narrow (Fig. 4K); (1) wide (Fig. 4L, M) (CI: 1.0, RI: 1.0).

The propleuron is motile and attached to the notum at the level of the dorsal wall (Hlavac, 1975). It rotates, along with the coxa, around a notal condyle. The endopleuron is shifted anteriorly so that most of it is anterior to that above the exopleuron. The exo- and endopleura are developed ventrally resulting in the reduction of the trochantin (Hlavac, 1975).

50. *Mesocoxae*: (0) contiguous, not separated by mesosternum (Fig. 6T); (1) separated by mesosternum (Fig. 6U); (2) very widely separated by mesosternum (Fig. 6V) (CI: 0.40, RI: 0.72).

51. *Apex of mesotibia*: (0) with two principal spines (Fig. 7R); (1) with the medial principal spine absent (Fig. 7Q); (2) without principal spines (CI: 1.0, RI: 1.0).

The homology of the primary spines may be concluded based on an examination of the structure of their surface, which is transversely scalelike in principal spines but long-itudinally scratched in the remaining robust setae on the apical face of the tibia.

52. *Metacoxa*: (0) basally narrowed (Fig. 7A, B); (1) basally widened with the posterior margin produced posteriorly at base (Fig. 7C–F) (CI: 1.0, RI: 1.0).

53. *Apex of metacoxa, medial apophysis*: (0) absent (Figs 4P–S, 7A–D); (1) present, produced posteriorly (Figs 4O, T–V, 7E, F) (CI: 0.12, RI: 0.46).

54. *Metacoxa, secondary ostium produced by medial apophysis and posterior margin of metacoxa*: (0) open (Fig. 4O, U, V); (1) closed posteriorly (Figs 4T, 7E, F) (CI: 1.0, RI: 1.0).

55. *Metacoxa, marginal line of posterior margin*: (0) absent (Fig. 7E); (1) present (Figs 4O, 7C, F) (CI: 0.10, RI: 0.10).

56. *Metacoxa, marginal line of lateral margin*: (0) absent (Fig. 7B, D); (1) present (Figs 4O, 7C, E, F) (CI: 0.50, RI: 0.75).

57. *Metacoxa, submarginal line of anterior margin*: (0) present (Figs 4O, 7A–D, F); (1) absent (Fig. 7E) (CI: 0.50, RI: 0.50).
58. *Metatibia, interior setae on apical face*: (0) absent (Fig. 7J, K); (1) robust (Fig. 7L); (2) fine (Fig. 7M) (CI: 0.33, RI: 0.60).
59. *Metatibia, transversal carina on lateral face*: (0) complete (from dorsal to ventral margin) (Fig. 8J, K); (1) interrupted at middle (Fig. 8L) (CI: 0.33, RI: 0.60).
60. *Apex of metatibia (except of the principal spines)*: (0) with spines and/or setae (Figs 7J–M, 8H–L); (1) glabrous (Fig. 8G) (CI: 0.20, RI: 0).
61. *Apex of metatibia, principal spines*: (0) close to each other on medial face (subapical) in the middle of tibia (left and right side of tarsal articulation) (Fig. 7N, O); (1) widely separated on medial or apical face (subapical or apical) of left and right side of tarsal articulation (Fig. 8B–D); (2) ventrally and contiguously on apical face (Fig. 8F); (3) present with one ventroapical spine only (Figs 7P, 8A); (4) close to each other but separated on apical face, sublateral in respect to tarsal articulation (Fig. 8E) (CI: 0.40, RI: 0.73).

The homology of the principal spines may be derived from their cuticular structure possessing a transversely reticulate surface (Fig. 4N, see character 51).

62. *Meso- and metatarsal claws*: (0) simple (Fig. 8M); (1) with a basal or median tooth ventrally (Fig. 8N, R, S); (2) with a median lobe ventrally (Fig. 8Q); (3) not toothed ventrally but incised apically (Fig. 8O) (CI: 0.37, RI: 0.75).
63. *Tarsal claws ventrally*: (0) without membranous fringe (Fig. 8M–R); (1) with membranous fringe (Fig. 8S) (CI: 1.0, RI: 1.0).
64. *Meso- and metatarsal claws*: (0) symmetrical (Fig. 8M, N, Q–S); (1) asymmetrical (Fig. 8O, P) (CI: 0.50, RI: 0.66).
65. *Meso- and metatarsal claws*: (0) immotile (Fig. 8M, N, Q–S); (1) motile (Fig. 8O, P) (CI: 0.50, RI: 0.66).

Elytra

66. *Elytral shelf*: (0) on a lower level in contrast to elytral surface (Fig. 5B, J, K); (1) on the same level as elytral surface (Fig. 5A, C) (CI: 1.0, RI: 1.0).

The transverse groove separating the mesoscutum and mesoscutellum is continued on the elytron as the elytral shelf, a depressed, shallowly grooved, area that receives the posterior edge of the postnotum when the elytra are closed (Doyen, 1966).

67. *Elytral base, apex of the subcostal basivenale*: (0) produced (Fig. 5A–C, H–L); (1) reduced in length (Fig. 5D, E, arrow) (CI: 1.0, RI: 1.0).
68. *Elytral base, anterior margin (in dorsal view)*: (0) not sinuate (Fig. 5A–F, H–L); (1) sinuate (Fig. 5G) (CI: 0.50, RI: 0.75).
69. *Elytral base, distance from apex of humeral plate to apex of subcostal basivenale (in respect to length of anterior margin)*: (0) small (Fig. 5D–L); (1) large (Fig. 5A, C) (CI: 1.0, RI: 1.0).
70. *Elytral base, anterior margin (dorsal view)*: (0) hook-like, elevated (Fig. 5H, arrow); (1) convex (Fig. 5A, C, G, J, L, arrow); (2) straight or concave (Fig. 5D–F, K) (CI: 0.33, RI: 0.80).
71. *Elytral base, radio-medial suture basally*: (0) moderately curved (Fig. 5H, J); (1) almost straight (Fig. 5D–G, K); (2) strongly curved (Fig. 5A, C, L) (CI: 0.16, RI: 0.58).
72. *Elytral base, anal lobe* (Larsén, 1966): (0) completely developed (Fig. 5A, B, F, H, J); (1) posteriorly reduced (Fig. 5E) (CI: 1.0, RI: 1.0).

The origin of the anal lobe is difficult to reconstruct, it is probably primarily derived from the cubital basivenale.

Hind wing

73. *Anterior border of the ala distal of apical hinge*: (0) glabrous (Fig. 5M); (1) completely setose (Fig. 5T); (2) setose behind apical hinge (Fig. 5N) (CI: 0.28, RI: 0.58).
74. *Wing vein RA_3 and RA_4 in basal third*: (0) strongly divergent, RA_4 in basal third strongly bent (Fig. 5O, T); (1) subparallel (Fig. 5P–R); (2) weakly divergent, RA_4 in basal third weakly bent (Fig. 5S) (CI: 0.66, RI: 0.93).
75. *Wing vein RA_3 and RA_4 apically*: (0) separated (Fig. 5O, Q, S, T); (1) fused or contiguous (Fig. 5P, R) (CI: 0.50, RI: 0.90).
76. *Wing vein RP_1*: (0) contiguous with RP_2 basally (Fig. 5O, S); (1) basally reduced, widely separated from RP_2 (Fig. 5P–R, T) (CI: 0.33, RI: 0.88).
77. *Wing vein RP_1 apically*: (0) convergent with RA_4 (see Kukalová-Peck & Lawrence, 1993: 238, fig. 52); (1) convergent and confluent with RA_4 (Fig. 5O, P, R–T); (2) subparallel with RA_4 (Fig. 5Q) (CI: 1.0, RI: 1.0).
78. *Ratio RA_3/RA_4*: (0) distinctly larger than 1.0 (Fig. 5O, Q, S); (1) approximately 1.0 (Fig. 5P, R, T); (2) little larger than 1.0 (CI: 0.66, RI: 0.90).
79. *Wing, anterior anal vein (AA)*: (0) straight (Fig. 5R); (1) convexly curved or bluntly bent (Fig. 5Q, U); (2) acutely bent (Fig. 5O) (CI: 0.50, RI: 0.66).

Abdomen

80. *Abdominal sternite 7 (penultimate ventrally visible sternite) posteriorly*: (0) with a narrow membrane (Fig. 10B, C); (1) with a very broad membrane (Fig. 10A); (2) without membrane (Fig. 10D) (CI: 0.25, RI: 0.45).

The numeration of the abdominal sternites by different authors does not reflect the homology of these segments (e.g. Mikšić, 1976; Sanmartín & Martín-Piera, 2003) due to the reduction of sclerotization in the basal abdominal segments. Krell (1996) examined the musculature of the ectodermic genitalia and provided clear terminology for the homology of the abdominal segments.

81. *Abdominal sternites ventrally*: (0) separated (Figs 9A, 10A–D); (1) medially fused (Fig. 9B); (2) completely fused (CI: 0.50, RI: 0.33).
82. *Propygidium and sternite 7*: (0) completely separated (Fig. 9C); (1) partially fused at base (Fig. 9D); (2) completely fused (Fig. 9E) (CI: 0.22, RI: 0.50).

Genitalia (genital segment, both sexes)

83. *Ninth tergite*: (0) convex or subrectangular, without any process at basal margin (Fig. 9J); (1) with two processes at basal margin (Fig. 10E) (CI: 1.0, RI: 1.0).

Male genitalia

84. *Spiculum gastrale (ventrale), vestigial (ninth) sternite*: (0) present (Fig. 9F–K); (1) absent (Fig. 9L) (CI: 1.0, RI: 1.0).

As a ventral part of the genital segment, which is derived from the ninth abdominal segment, the spiculum gastrale consists of a cranial and a caudal portion. The cranial portion is interpreted by Hieke (1966) to be derived from lateroventrally displaced and secondarily cranially fused tergal apodemes IX. The caudal portion, which Sanmartín & Martín-Piera (2003) termed 'vestigial sternite', presumably originates from sternite IX (Krell, 1996).

The vestigial (ninth) sternite is also analogously absent or reduced in some representatives of Rutelinae and Dynastinae, such as *Parastasia* and *Cyclocephala* (Jameson, 1998).

85. *Spiculum gastrale, basally widened piece*: (0) at least half as long as wide (Fig. 9F–J); (1) considerably shorter than wide (Fig. 9K, L) (CI: 0.25, RI: 0.86).

86. *Spiculum gastrale, cranial apex*: (0) not produced (Fig. 9F–H); (1) moderately produced (process approximately as long as widened basal portion) (Fig. 9J); (2) strongly produced (process more than twice as long as widened basal portion) (Fig. 9K, L) (CI: 0.15, RI: 0.47).

87. *Spiculum gastrale, cranial process*: (0) broad and dorsoventrally flattened (Fig. 9F–K); (1) throughout filiform, very slender and circular in cross-section (Fig. 9L) (CI: 1.0, RI: 1.0).

According to Jameson (1998), character state 1 also occurs in some ruteline genera, such as *Rutela* and *Pelidnota*. However, it should be considered as an analogous development to that within the sericine lineages.

88. *Aedeagus, sclerotized plates at apex of ventral phallobase*: (0) absent (Fig. 11B–E, M–O); (1) present (Fig. 11A, F, L, P–S) (CI: 0.25, RI: 0.84).

89. *Aedeagus, sclerotized plates at apex of ventral phallobase*: (0) separated (Figs 10F–K, 11R); (1) fused with each other (Fig. 11L, Q, P); (2) fused with each other and with lateral lamina of phallobase (Fig. 10L) (CI: 0.40, RI: 0.70).

90. *Aedeagus, basal ostium of phallobase*: (0) large (at least half as long as phallobase) (Fig. 11L–R); (1) small (less than half as long as phallobase) (Figs 10F, G, L, 11G–K, S) (CI: 0.33, RI: 0.90).

91. *Phallobase ventrally*: (0) membranous (Figs 10F, 11M–O, Q, R); (1) sclerotized, initiating from lateral lamina of phallobase (Figs 10G, J, L, 11K, S); (2) ventral plates enlarged basally, sclerotized along midline too (Fig. 11P) (CI: 0.28, RI: 0.66).

92. *Phallobase ventrally, lateral lamina at level of distal border of basal ostium*: (0) unarmed or convex (Fig. 11B–E); (1) with robust hooklike structure (Figs 10N, P, 11G, S); (2) with blunt tooth (Figs 10L, M, 11F, H, J) (CI: 0.33, RI: 0.78).

93. *Parameres apically*: (0) glabrous (Figs 10J, P, 11B, F, K–P); (1) setose (Figs 10H, O, 11Q) (CI: 0.25, RI: 0.70).

94. *Endophallus, temones*: (0) present (Fig. 12A–D, F–H); (1) absent (Fig. 12E) (CI: 0.50, RI: 0).

The temones are a paired, elongate, endophallic sclerite articulating to the base of the median lobe and extending into the basal piece (phallobase) (D'Hotman & Scholtz, 1990). Krell (1996) pointed out that in Lamellicornia, homologization of endophallic sclerites is far from resolved. Consequently he termed the 'temones' neutrally as 'proximal endophallic sclerite'. However, the location in the endophallus seems a rather suitable criterion for homology of the endophallic sclerites within Scarabaeidae.

95. *Endophallus, temones*: (0) long and slender (Fig. 12A–D, F); (1) short and wide (Fig. 12G, H) (CI: 0.25, RI: 0.72).

96. *Endophallus, v-shaped piece*: (0) present and fully developed (Fig. 12A–C); (1) absent (Fig. 10O); (2) strongly reduced (Fig. 12E, G, H) (CI: 0.33, RI: 0.78).

The term 'v-shaped piece' was introduced by Sanmartín & Martín-Piera (2003). It represents the caudal portion of the caudally convergent temones (proximal endophallic sclerite), which is situated ventrally on the endophallus. In Scarabaeidae, the v-shaped piece may be fused or separated with the cranial portion of the temones, which apically are stretched out along the dorsal face of the endophallus.

97. *Endophallus, v-shaped piece and temones*: (0) fused (Fig. 12A–D, F); (1) separated (Fig. 12D, F–H) (CI: 0.12, RI: 0.41).

Female genitalia

98. *Glandulae accessoriae*: (0) absent (Fig. 12J, K); (1) present (Fig. 12L–N); (2) secondarily reduced (uninformative).

Because the monophyly of Aphodiinae + Scarabaeinae (represented by *Aphodius* and *Copris*, respectively, in this study) has been shown in several studies by a number of apomorphies (e.g. Browne & Scholtz, 1998), I have coded the loss of the accessory glands in *Copris* (Scarabaeinae) as a independent character state to retain a higher tree resolution.

99. *True styli*: (0) present (Fig. 12J, K); (1) absent (Fig. 12L–N) (CI: 0.50, RI: 0).

According to Tanner (1927), the styli are not homologous to the so-called 'genital palps' (or vaginal palps, e.g. Krell, 1996). As suggested by Sanmartín & Martín-Piera (2003), the latter are derived from coxite of the ninth segment. Holloway (1972) presented a hypothesis that the styli including their basal hemisternites (e.g. in Trogidae and Lucanidae) are derived from the tenth segment. However, she provided no evidence for this assumption. According to the studies of Tanner (1927), the following sclerites and their respective terminology used in some later works are homologous (e.g. Coca-Abia & Martín-Piera, 1991; Sanmartín & Martín-Piera, 2003): proctiger (= vestigial tergite 1), paraproct (= vestigial tergite 2), valvifer (= vestigial sternite).

100. *Sclerotized portion of valvifer*: (0) present (Fig. 12J–L); (1) absent (Fig. 12M, N) (CI: 0.20, RI: 0.77).

101. *Glandulae accessoriae*: (0) left and right glandulae lead separately to the vagina (Fig. 12L, M); (1) left and right glandulae with a common duct leading to the vagina (Fig. 12N) (CI: 1.0, RI: 1.0).

102. *Membranous anal fold between eighth and ninth segments (ventral view)*: (0) large (enclosing the glandulae accessoriae if present) (Fig. 12J–L); (1) small or absent leaving the glandulae accessoriae free (Fig. 12M, N) (CI: 0.20, RI: 0.75).

Larva

Larval characters are not well represented herein owing to the lack of available material and the poor taxonomic exploration of immature stages resulting in the fact that the larvae of numerous scarab lineages remain undescribed. On the other hand, Grebennikov & Scholtz (2004) encountered difficulties in interpreting the morphology of certain larval structures in Scarabaeoidea for phylogenetic purposes due to their 'high adaptive value' of characters or due to their uncertainty of homology.

103. *Galea*: (0) with two joints (Fig. 13A); (1) with one joint (Fig. 13B–D) (uninformative).
104. *Haptomerum (epipharynx), number of heli*: (0) three or four (Fig. 13E); (1) more than five (Fig. 13G, H); (2) less than two (Fig. 13F) (CI: 0.28, RI: 0.58).
105. *Galea and lacinia*: (0) entirely separated (Fig. 13A, B); (1) fused but with a complete suture (suture may be absent basally) (Fig. 13C); (2) entirely fused, without suture (Fig. 13D) (CI: 1.0, RI: 1.0).
106. *Anal split*: (0) y-shaped, medially deeply incised (Fig. 13J, M, O, Q); (1) medially moderately incised (Fig. 13N); (2) simply transverse (Fig. 13K, L, P) (CI: 0.40, RI: 0.75).
107. *Palidium (last sternite)*: (0) absent (Fig. 13J–M); (1) transverse and arched (Fig. 13Q); (2) transverse and angled (Fig. 13O); (3) longitudinal and straight (one row of setae) (Fig. 13N, P) (CI: 0.50, RI: 0.50).

The palidium is part of the raster on the last abdominal sternite of larvae. Cribb *et al.* (1998) revealed that this raster is a complex of mechanoreceptive setae. Their chemical and morphological investigations did not provide any evidence that the raster is a site for chemical emissions. The ultra-structure of the setae of palidium (pali) have shown that each seta is innervated by a single dendrite that ends in a tubular body at the base of the seta. Due to the limited number of taxa examined by Cribb *et al.* (1998), there is no indication as to how pali differ from normal setae of the ventral surface of the last abdominal sternite, and whether the pali within the diverse phytophagous lineages are truly homologous.

Results

The analysis of 107 adult and larval characters with the parsimony ratchet and the above-mentioned settings yielded 109 equally parsimonious trees of 426 steps (CI 0.36, RI 0.76). Repeating the search ten times, the same statistics as above were obtained. Characters 98 and 103 were uninformative in the present dataset. The strict consensus of these trees, with jackknife values and Bremer support, is presented in Fig. 14, with areas of topological conflict shown as polytomies. Repeating the parsimony ratchet with modified settings (1000 iterations and ten trees hold per iteration with ten sequential ratchet runs) resulted in an increasing number of equally parsimonious trees without an altered topology in the strict consensus tree. The tree topology was unaffected by altering acctran or deltran optimizations.

In some cases, data for the characters of thoracic musculature and larval morphology were missing. To test the sensitivity of the results to missing data, additional analyses were run: one omitting characters 42–45, which resulted in no alteration of consensus topology of the full analysis, and a second deleting characters 42–45 and 103–107 from the analysis. These analyses were run using the same settings for the parsimony ratchet and yielded ninety equally parsimonious trees of 399 steps (CI 0.35, RI 0.76).

The strict consensus (Fig. 15) shows a similar topology to the consensus tree of the first analysis (Fig. 14) with all characters included. The positions of a few taxa are different, including Phyllotocini (*Phyllotocus* + *Anthotocus*) and *Diphucephala*, and the clade comprising *Aphodius* + *Copris* is no longer monophyletic. Because data on larval morphology were available for most principal lineages, and the alteration in the topology excluding larval characters was minimal, further discussion will be based only on the full character analysis. Figure 16 illustrates unambiguous character changes along each branch of the consensus tree from the first analysis (with all characters included), which was used for the following discussion of the apomorphies and the character evolution of groups and lineages.

The strict consensus tree (Fig. 14) reveals six major clades: (1) the 'aphodiine line' (Browne & Scholtz, 1998) including *Aphodius* + *Copris*; (2) the orphnine clade here containing *Orphnus*; (3) *Hoplia*; (4) Phyllotocini including *Phyllotocus* + *Anthotocus*; (5) the 'melolonthine group I' (node D, Fig. 14) including *Acoma, Amphimallon, Chasmatopterus, Elaphocera, Europteron, Macrophylla, Melolontha, Pachypus, Propomacrus, Tanyproctus, Xylonichus*, and the 'ruteline subgroup' of Browne & Scholtz (1998) represented by *Oryctes, Adoretus, Anisoplia, Anomala, Trichius, Osmoderma, Protaetia*, and *Valgus*; as well as (6) the 'melolonthine group II' (node C, Fig. 14) containing *Athlia, Diphucephala, Heteronyx, Sericoides, Telura*, Ablaberini, and Sericini.

Discussion

Monophyly of the 'orphnine group' + 'melolonthine group'

The results strongly support the monophyly of the 'orphnine group' (including the Orphninae represented in this study by a single taxon *Orphnus*) + a 'melolonthine group'. The latter clade traditionally includes groups of phytophagous scarabs such as Dynastinae, Hopliinae, Melolonthinae, Rutelinae, and Cetoniinae. Both clades were also found to form a monophyletic clade by Browne
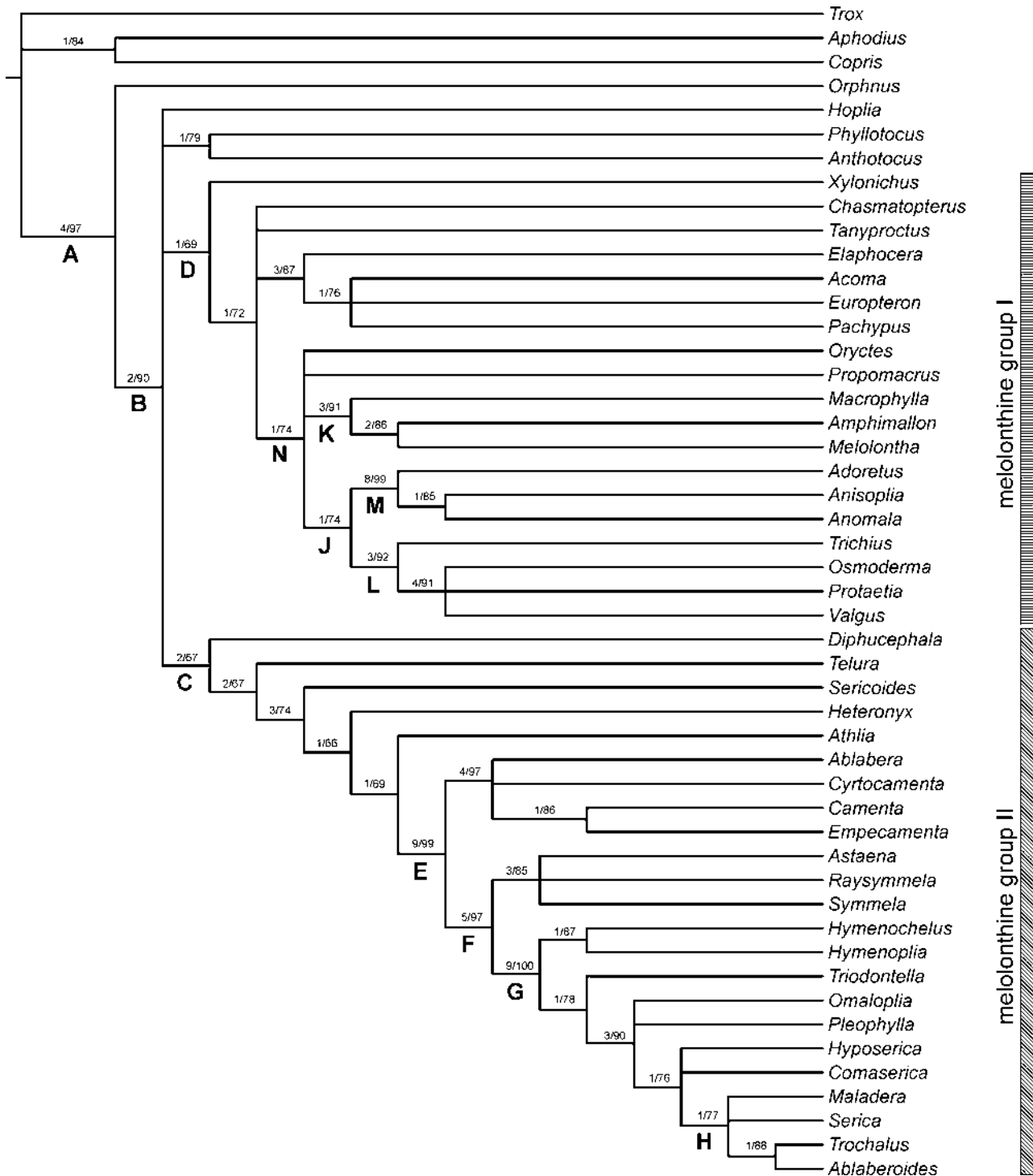
Fig. 14. Strict consensus of 109 equally parsimonious trees with a length of 426 steps (consistency index = 0.36 and retention index = 0.76); above each branch are support indices (Bremer support/jackknife values).
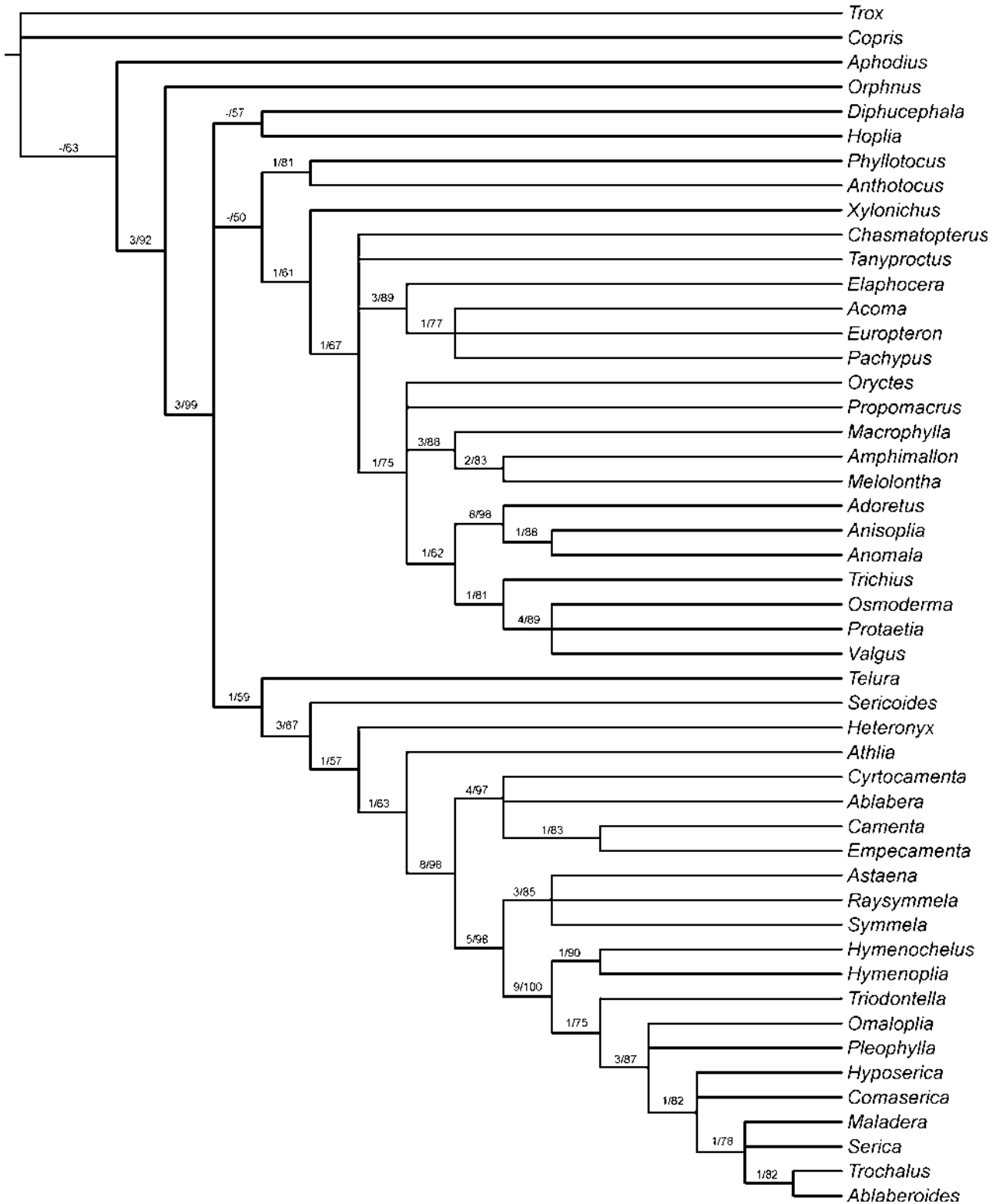
Fig. 15. Strict consensus of ninety equally parsimonious trees with a length of 399 steps (consistency index = 0.35 and retention index = 0.76), with characters of thoracic musculature (characters 42–45) and larval morphology (characters 103–107) excluded from the analysis; above each branch are support indices (Bremer support/jackknife values).

& Scholtz (1998). In the present study, the monophyly of these two groups is based on five nonhomoplasious synapomorphies (Fig. 16, node A): (1) a short and straight dorsal process (p1) of the mesofurcal arm (31: 1); (2) the mesofurcal arm with an apically narrowed dorsal process (p1) (32: 1); (3) metacoxa basally widened with the posterior margin produced posteriorly at the base (52: 1); (4) haptomerum of the epipharynx (larvae) with three or four heli (104: 0); (5) galea and lacinia of the larvae fused (at least partially) (105: 1).

This sister-group relationship of the 'orphnine group' and the 'melolonthine group' provides an interesting case of a high asymmetry in species diversity within Scarabaeoidea. Whereas the 'orphnine group' (Orphninae) represents a small group with a few genera and species, the 'melolonthine group' is the lineage with the greatest species diversity within the Scarabaeoidea, containing tens of thousands of species. Most taxa in this lineage feed on angiosperms (Scholtz & Chown, 1995), which could be taken to imply that the successful evolution of melolonthine scarabs relates to the huge radiation of these plants, although the mechanisms provoking that development are still unexplored.

Monophyly of the 'melolonthine group'

This clade (node B; Bremer support 2, jackknife 90%) is based on at least five apomorphies (Fig. 16): (1) galea with one joint (9: 1); (2) the distally shortened lacinia not extending beyond the basis of the galea (12: 1); (3) the palpiger enclosed by the prementum and the ligular lobe (18: 1); (4) wing vein RA_3 and RA_4 in the basal third strongly divergent, with RA_4 strongly bent caudally in the basal third (74: 0); (5) the large basal ostium of the phallobase at least half as long as the phallobase (90: 0). The latter character is reversed in Sericini and the representatives of Rutelinae included in this analysis where the basal ostium of the phallobase is small, similar to the outgroup (*Trox*) and to the lineage *Aphodius + Copris*. I consider the small or lacking incision between caudal lobes of the postnotum (metathorax, 38: 1) a less suitable character (CI 0.25) to support the clade, as its development might depend on the specimen's weight and size, although it evolved independently from the size of the postnotal lobes (character 37). The 'melolonthine group' comprises two major melolonthine clades (melolonthine groups I and II, nodes C and D, Fig. 14) and two minor lineages (*Hoplia* and *Anthocus + Phyllotocus*).

Monophyly of Sericini

The results of this cladistic analysis support the monophyly of the Sericini. At node F (Bremer support 5, jackknife 97%) the following nonhomoplasious apomorphies support this clade: (1) vestigial (ninth) sternite in the spiculum gastrale absent (84: 1); (2) cranial process of the spiculum gastrale filiform, very slender and circular in cross-section (87: 1); (3) glandulae accessoriae with left and right glandulae (1+2) having a common duct to the

vagina (101: 1). The small basal ostium of the phallobase (90: 1, character reversal from node A) and the enlarged metacoxa (46: 1) are important apomorphies of the Sericini. The latter character state is also found in *Phyllotocus*, a genus often placed among the Sericini (e.g. Dalla Torre, 1912; Britton, 1957; Machatschke, 1959; Houston & Weir, 1992).

Monophyly of Sericini + Ablaberini

In concordance with Machatschke (1959), this analysis identified Ablaberini as the sister to Sericini. The monophyly of Sericini + Ablaberini (node E) is supported by one nonhomoplasious apomorphy: the ninth tergite having two sharply pointed processes at its cranial margin (83: 1). The node (E) is also supported by at least eight further apomorphies (Bremer support 9, jackknife 99%), such as the completely fused labrum and clypeus (1: 1) having a common continuous lateral margin (2: 1), the galea having eight teeth (6: 2) of which four are visible in ventral view (on maxilla) (10: 0), the absence of the marginal line of the posterior margin of the metacoxa (55: 0), the basally widened piece of the spiculum gastrale, which is considerably shorter than wide (85: 1), the present sclerotized plates at the apex of the ventral phallobase of the aedeagus (88: 1), the lateral lamina of the ventral phallobase at the level of the distal border of the basal ostium with the blunt tooth (92: 2), and with apically setose parameres (93: 1).

Evaluation of clades within 'melolonthine group I'

'Melolonthine group I' shares several apomorphies at node D, with only one being nonhomoplasious (40: 1). The included taxa of Melolonthini (node K), Cetoniinae (node L) and Rutelinae (node M) are strongly supported as being monophyletic. However, as in Sanmartín & Martín-Piera (2003) (e.g. *Sparrmannia*), some of the taxa (e.g. *Macrophylla*) classified as Pachydemini (Dalla Torre, 1912; Lacroix, 2000), are placed by this analysis with the genera of Melolonthini. The relationships of Dynastinae (*Oryctes*) and Euchirinae (*Propomacrus*) were not sufficiently resolved with the data matrix used in this analysis. The topology of the clade of 'melolonthine group I' is surprising with the nesting of the Melolonthini (*Macrophylla* (*Amphimallon*, *Melolontha*)) within the 'ruteline subgroup' (Browne & Scholtz, 1998) (node N), which is supported by two apomorphies: (1) the apically fused or contiguous RA_3 and RA_4 (75: 1) and (2) by equally long RA_3 and RA_4 (ratio RA_3/RA_4 approximately 1.0) (for further details consult Fig. 16). Interestingly, *Chasmatopterus* (Chasmatopterini) and *Pachypus* (Pachypodinae) are grouped closely with representatives of Pachydemini (*Tanyproctus*, *Elaphocera*, *Europteron*). In 93% of the maximum parsimonious trees, this clade is the sister group (see Fig. 17) of the 'ruteline subgroup'. In the phylogeny of Browne & Scholtz (1998), Dynastinae (represented in this analysis by *Oryctes*) + Rutelinae (*Adoretus* (*Anisoplia*, *Anomala*)) is monophyletic, which is supported
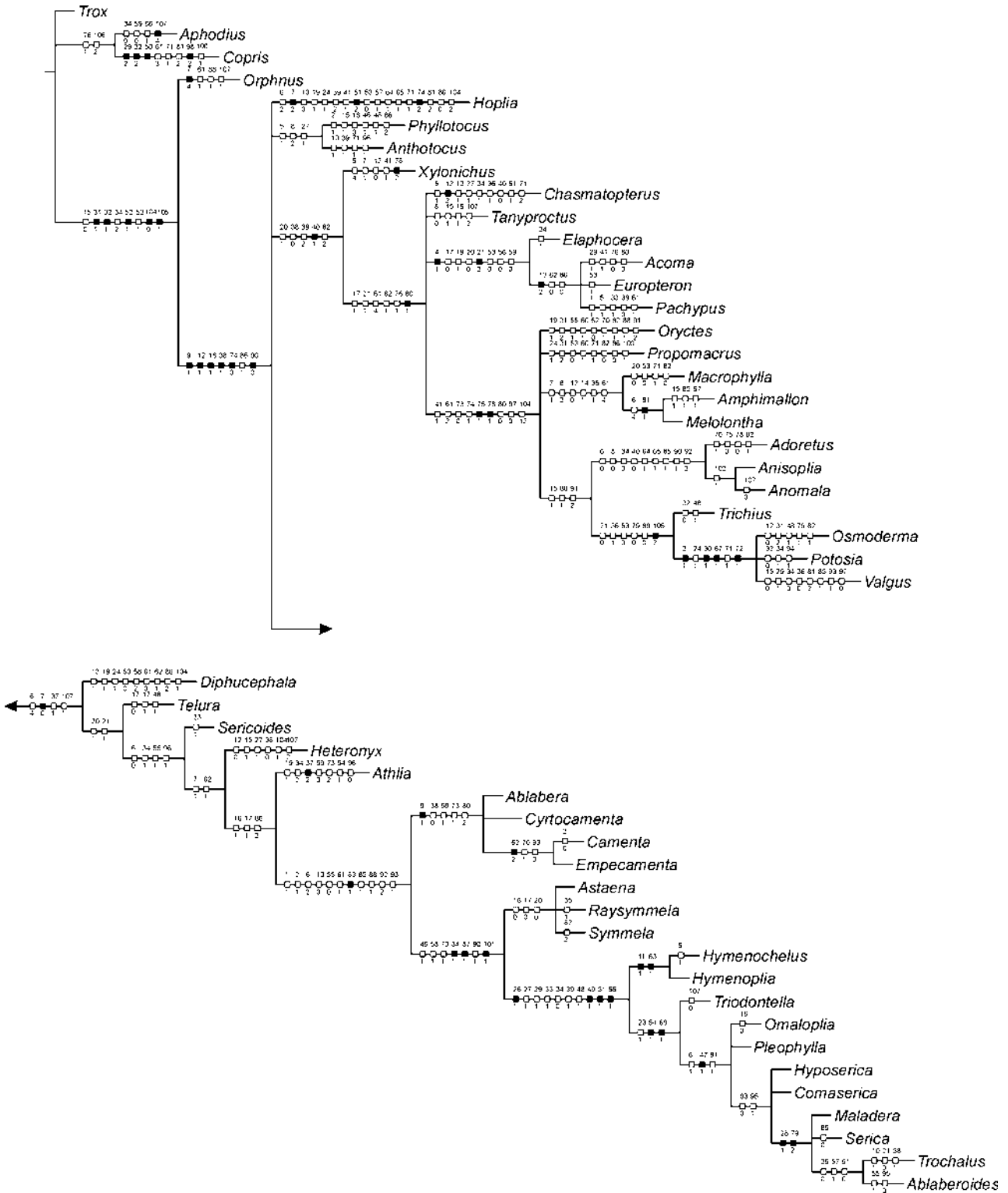
Fig. 16. Strict consensus of 109 equally parsimonious trees with a length of 425 steps (consistency index = 0.36 and retention index = 0.76) showing character changes and apomorphies mapped by state (only discontinuous states are mapped as homoplasy and just unambiguous changes are shown, unsupported nodes collapsed and using proportional branch lengths). Solid squares: nonhomoplasious character states; open squares: homoplasious character states).

by a number of synapomorphies in the hind wing articulation. This close relationship was not seen in the results of this analysis. Because characters used in this analysis were chosen to reconstruct the phylogeny of Sericini, the relationships of the taxa outside this clade should be regarded as preliminary, as they may change with the insertion of characters more appropriate for investigating relationships among these taxa.

Phylogenetic position and biogeographical history of Sericini

The Sericini + Ablaberini are nested within a clade of taxa with a distribution primarily in southern continents (here preliminarily termed 'melolonthine group II'). This clade is supported by a small number of apomorphies (node C; 6: 4, 7: 0, 37: 1, 107: 1, Fig. 16). The closest relatives of Sericini + Ablaberini are *Athlia* (southern South America) and *Heteronyx* (Australia) (Britton, 2000), which have the following apomorphies: (1) all teeth completely fused with the galea (7: 1) and (2) meso- and metatarsal claws with a basal or median tooth ventrally (62: 1). From the pectinate structure of the topology of this clade, one could assume that Sericini + Ablaberini are derived from one of these southern lineages (*Diphucephala*, *Telura*, *Sericoides*, *Heteronyx*, *Athlia*). This hypothesis is consistent with the idea of several authors classifying the Australian and southern American melolonthine lineages into separate tribes (Diphucephalini, Scitalini, Sericoidini, Heteronycini; cf. Britton, 1957; Houston & Weir, 1992; Evans, 2003). Because these lineages do not occur in the Palaeotropics or Nearctic, it is plausible that the ancestors of Sericini + Ablaberini and *Athlia* were separated by a vicariance event, such as the separation from Gondwana and the northern drift of the African plate, where Sericini and Ablaberini probably diversified during the early Tertiary, with a dispersal of the most ancestral Sericini over the Atlantic to South America. Similar dispersals are hypothesized and well documented in other groups of animals, such as primates or rodents (e.g. Simpson, 1980; Takai *et al.*, 2000). The clade containing *Astaena*, *Raysymmela*, and *Symmela* was restricted to tropical South America and moved north into Central America (as far as Nicaragua) during the late Tertiary. The monophyly of holarctic–palaeotropical Sericini (node G; Bremer support 9, jackknife 100%) is best supported by numerous unambiguous apomorphies, such as (1) a large interior process (p3) of the mesofurcal arm (26: 1); which is (2) lobiform in shape (34: 0); (3) the medially separated mesofurcal arms (27: 1); (4) the small and conical craniomedial surface of the mesofurcal arm (19: 1); (5) the absence of an anterior process (p2) of the mesofurcal arm (33: 1); (6) the evenly divergent anterior and posterior margin of the ventral median flange of the metendosternite (lateral view) (39: 1); (7) the absence of a procoxal transversal carina (48: 1); (8) the wide fusion of the proexopleura and trochantin (49: 1); (9) the apex of the mesotibia with one reduced principal spine (51: 1); and (10) the elytral shelf being on the same level as the elytral surface (66: 1). Evidence for a radiation of this clade on the

African plate includes the fact that most extant ancestral lineages (*Triodontella*, *Hymenoplia*, *Pleophylla*, *Omaloplia*) of the holarctic–palaeotropical Sericini (node G) presently occur just in the Afrotropical region and the western Mediterranean, whereas the more apical lineages (node H) also occur in Asia and North America (*Maladera*, *Serica*). These 'Modern Sericini' share some important unambiguous apomorphies, such as the presence of a carina from the craniolateral margin of the mesosternum to the mesofurcal arm (28: 1) and the acutely bent anterior anal vein (AA) (79: 2).

It is very difficult to place the oldest known fossils of melolonthine lineages into this phylogeny, as it is impossible to observe most of the characters used. In the case of the Lower Cretaceous fossil genus *Lithanomala* (Nikolaev, 1998), it has only one diagnostic character (the position and shape of the labrum + clypeus), which could place it in at least two vastly different positions in the phylogenetic tree. Similarly, *Cretoserica* (Nikolaev, 1998; Krell, 2000) has at least four alternative positions throughout the 'melolonthine group' clade. According to the fossil record, the more derived sericine lineages, such as '*Serica*' and '*Maladera*' from North America and Central Europe can be dated to at least the Oligocene using fossils (Krell, 2000), which corresponds with the evolutionary hypothesis of Sericini formulated above. For a more detailed biogeographical analysis, it will be necessary to explore the Sericini phylogeny in the context of the role of Madagascar and the Indian plate in the evolution of the group, and consequently to consider a wider range of the more than 200 described sericine genera.

Considerations for the classification of melolonthine lineages

The reconstructed phylogeny of the melolonthine lineages have implications for the present scarabaeoid classification. According to the consensus tree (Fig. 14), the Melolonthinae (or Melolonthidae, cf., e.g. Baraud, 1992; Lacroix, 2000) in their current form (including all taxa of node B, excluding those of node N, but including those taxa united in node K, e.g. Evans, 2003) is paraphyletic. This would also be consistent with the difficulty in finding apomorphies for this group (Browne & Scholtz, 1998). The results of the analysis (Fig. 14) corroborate the paraphyly of the tribe Pachydemini. Sanmartín & Martín-Piera (2003) also discovered that the monophyly of Pachydemini is not well supported. The representatives of Chasmatopterini (*Chasmatopterus*) and Pachypodinae (*Pachypus*) are nested within the Pachydemini and the node of *Chasmatopterus*, *Tanyproctus* (*Elaphocera* (*Acoma*, *Europteron*, *Pachypus*)) collapsed to a polytomy that included 'melolonthine group I' in the strict consensus tree (Fig. 14). Consequently, it appears that Pachydemini should be redefined, once a more robust phylogenetic analysis has been performed on this tribe. Regarding the 'Sericinae', I refrain from expanding the term for a wider range of lineages than Sericini + Ablaberini, as some authors do (e.g. Britton, 1957; Lacroix, 2000), because some of the relationships need further detailed studies before they can be applied persistently to the classification of the group.
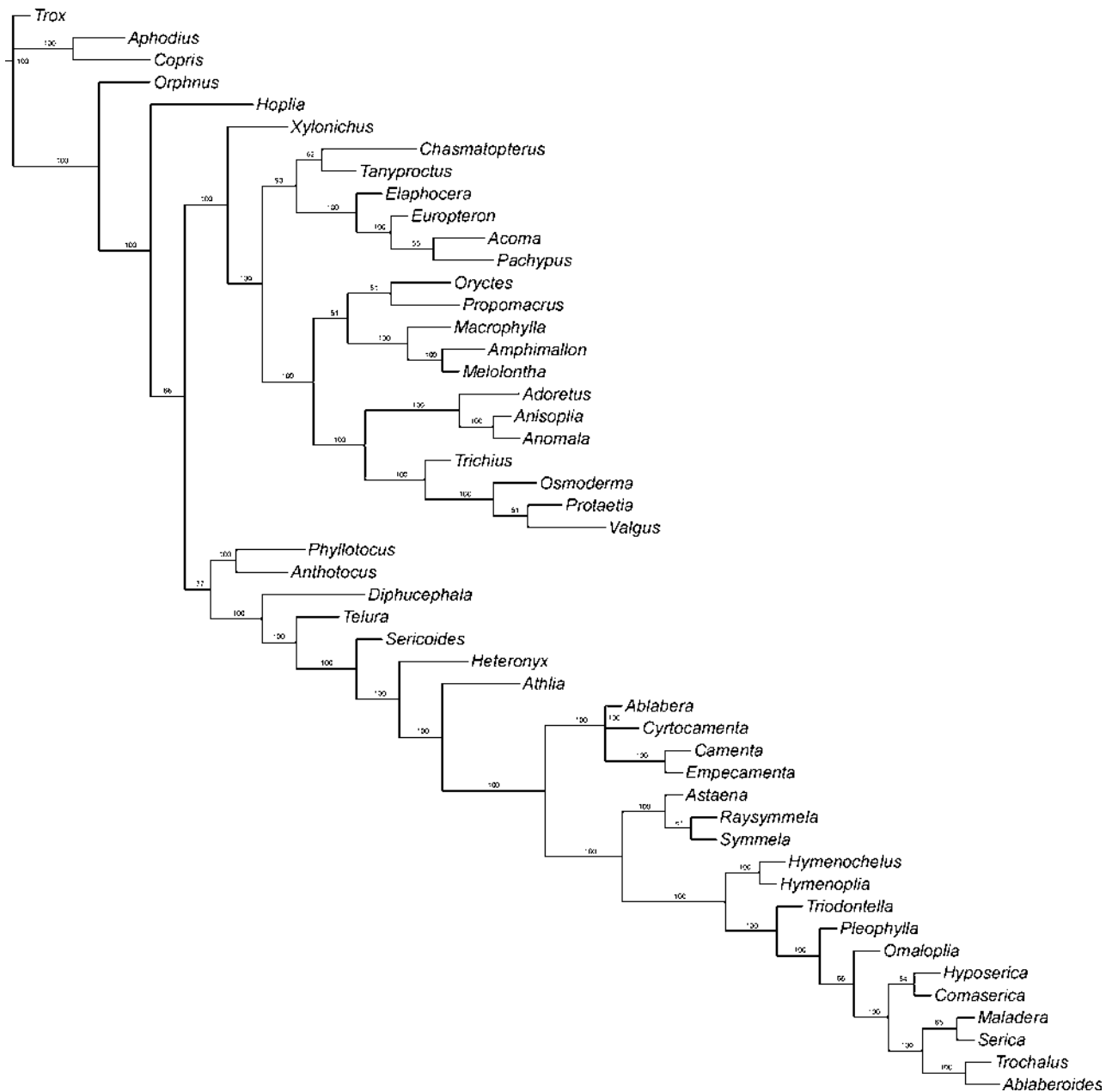
Fig. 17. Majority rule consensus tree generated with WINCLADA showing unsupported nodes collapsed and using the proportional branch lengths. The numbers above the branches indicate the frequency of the node among all maximum parsimonious trees.

Regarding the exclusion of *Athlia* from Sericini, it is premature to erect a new tribe for this genus until more detailed studies are made to explore the relationships between southern hemispheric melolonthine lineages.

Supplementary material

A Nexus file of the data matrix is available from: http://www. blackwellpublishing.com/products/suppmat/SEN/SEN307/ SEN307sm.htm

Acknowledgements

References

Anderson, W.H. (1936) A comparative study of the labium of coleopterous larvae. *Smithsonian Miscellaneous Collections*, **95**, 1–29.

Baraud, J. (1992) Coléoptères Scarabaeoidea d'Europe. *Faune de France, France et Regions Limitrophes*, **78**, 1–856.

Beutel, R.G. (1994) Phylogenetic analysis of Hydrophiloidea (Coleoptera: Polyphaga: Staphyliniforma) based on characters of adults and larvae. *Koleopterologische Rundschau*, **64**, 103–131.

Beutel, R.G. (1997) Über Phylogenese und Evolution der Coleoptera (Insecta), insbesondere der Adephaga. *Abhandlungen des Naturwissenschaftlichen Vereins in Hamburg (NF)*, **31**, 1–164.

Beutel, R.G. & Haas, F. (2000) Phylogenetic relationships of the suborders of Coleoptera (Insecta). *Cladistics*, **16**, 103–141.

Bremer, K. (1988) The limits of amino acid sequence data in angiosperm phylogenetic reconstruction. *Evolution*, **42**, 795–803.

Bremer, K. (1994) Branch support and tree stability. *Cladistics*, **10**, 295–304.

Britton, E.B. (1957) *A Revision of the Australian Chafers (Melolonthinae)*, Vol. I. British Museum (Natural History), London.

Britton, E.B. (2000) A review of *Heteronyx* Guérin-Meneville (Coleoptera: Scarabaeidae: Melolonthinae). *Invertebrate Taxonomy*, **14**, 465–589.

Browne, J. & Scholtz, C.H. (1996) The morphology of the hind wing articulation and wing base of the Scarabaeoidea (Coleoptera) with some phylogenetic implications. *Bonner Zoologische Monographien*, **40**, 1–200.

Browne, J. & Scholtz, C.H. (1998) Evolution of the scarab hind-wing articulation and wing base: a contribution toward the phylogeny of Scarabaeidae (Scarabaeoidea: Coleoptera). *Systematic Entomology*, **23**, 307–326.

Browne, J. & Scholtz, C.H. (1999) A phylogeny of the families of Scarabaeoidea. *Systematic Entomology*, **24**, 51–84.

Coca-Abia, M. & Martín-Piera, F. (1991) Anatomy and morphology of the genitalia in the subtribe Rhizotrogini (Col. Melolonthidae, Melolonthini): taxonomic implications. *Advances in Coleopterology* (ed. by M. Zunino, X. Belles and M. Blas), pp. 61–78. Association European Coleopterology, Barcelona.

Crampton, G.C. (1926) A comparison of the neck and prothoracic sclerites throughout the orders of insects. *Transactions of the American Entomological Society*, **52**, 199–248.

Crampton, G.C. (1928) The eulabium, mentum, submentum, and gular region of insects. *Journal of Entomology and Zoology*, **20**, 1–20.

Cribb, B.W., Hull, C.D., Moore, C.J., Miller, L.J. & Yeates, D.K. (1998) Structure of raster in Melolonthine larvae. *Annals of the Entomological Society of America*, **91**, 202–210.

Crowson, R.A. (1944) Further studies on the metendosternite in Coleoptera. *Transactions of the Royal Entomological Society, London*, **94**, 273–310.

D'Hotman, D. & Scholtz, C.H. (1990) Phylogenetic significance of the structure of the external male genitalia in the Scarabaeoidea (Coleoptera). *Entomology Memoir, Department of Agricultural Development*, **77**, 1–51.

Dalla Torre, K.W. (1912) Scarabaeidae: Melolonthinae I. *Coleopterorum Catalogus*, **45**, 1–84.

Das, G.M. (1937) The musculature of the mouthparts of insect larvae. *Journal of Microscopical Science*, **80**, 39–80.

de Castro, A.V. (2001) The terminology of metendosternite in Coleoptera. *Elytron*, **15**, 191–194.

Dorsey, C.K. (1943) The musculature of the labrum, labium and pharyngeal region of adult and immature Coleoptera. *Smithsonian Miscellaneous Collections*, **103**, 1–42.

Doyen, J.T. (1966) The skeletal anatomy of *Tenebrio molitor* (Coleoptera: Tenebrionidae). *Miscellaneous Publications of the Entomological Society of America*, **22**, 103–150.

Evans, A.V. (2003) A checklist of the New World chafers (Coleoptera: Scarabaeidae: Melolonthinae). *Zootaxa*, **211**, 1–458.

Farris, J.S., Albert, V.A., Källersjö, M., Lipscomb, D. & Kluge, A.G. (1996) Parsimony jackknifing outperforms neighbor-joining. *Cladistics*, **12**, 99–124.

Giljarov, M.S. (1964) Semejstvo Scarabaeidae – Plastinchatousye. *Opredelitel' Obitajushzhich v Pocve Licinok Nasekomykh* (ed. by M. S. Giljarov), pp. 289–330. Nauka, Moskva.

Goloboff, P. (1999) *NONA*, version 2.0 Published by the author, Tucumán.

Grebennikov, V.V. & Scholtz, C.H. (2004) The basal phylogeny of Scarabaeoidea (Insecta: Coleoptera) inferred from larval morphology. *Invertebrate Systematics*, **18**, 321–348.

Hansen, M. (1997) Phylogeny and classification of the staphyliniform beetle families (Coleoptera). *Biologiske Skrifter*, **48**, 1–339.

Hieke, F. (1966) Vergleichende funktionelle Anatomie der Abdominalmuskulatur einiger männlicher Coleopteren unter besonderer Berücksichtigung des Genitoanalkomplexes. *Deutsche Entomologische Zeitschrift, NF*, **13**, 1–168.

Hlavac, T.F. (1975) The prothorax of Coleoptera (except Bostrichiformia-Cucujiformia). *Bulletin of the Museum of Comparative Zoology*, **147**, 137–183.

Holloway, B.A. (1972) The systematic position of the genus *Diphyllostoma* Fall (Coleoptera: Scarabaeoidea). *New Zealand Journal of Science*, **13**, 31–38.

Horion, A. (1958) *Faunistik der Mitteleuropäischen Käfer*, Band 6. Feyel, Überlingen-Bodensee.

Houston, W.W.K. & Weir, T.A. (1992) Melolonthinae. *Zoological Catalogue of Australia Coleoptera: Scarabaeoidea* (ed. by W. W. K. Houston). APGS, Canberra.

Howden, H.F. (1982) Larval and adult characters of *Frickius* Germain, its relationship to the Geotrupini, and a phylogeny of some major taxa in the Scarabaeoidea (Insecta: Coleoptera). *Canadian Journal of Zoology*, **60**, 2713–2724.

Iablokov-Khnzorian, S.M. (1977) Über die Phylogenie der Lamellicornia (Ins. Col.). *Entomologische Abhandlungen, Staatliches Museum für Tierkunde Dresden*, **41**, 135–200.

Jameson, M.J. (1998) Phylogenetic analysis of the subtribe Rutelina and revision of the *Rutela* generic groups (Coleoptera: Scarabaeidae: Rutelidae: Rutelini). *Bulletin of the University of Nebraska State Museum*, **14** (1997), 1–184.

Klausnitzer, B. & Krell, F.-T. (1996) Scarabaeoidea. *Die Larven der Käfer Mitteleuropas 3 Bd, Polyphaga*, Teil 2 (ed. by B. Klausnitzer), pp. 11–89. Goecke & Evers, Krefeld.

Krell, F.-T. (1992) Verschmelzung von Antennomeren (Symphysocerie) als Regelfall bei *Temnorhychus repandus* Burm., 1847, sowie phylogenetische, taxonomische, faunistische und nomenklaturische Anmerkungen zu diversen Taxa dieser Gattung (Pentodontini). *Deutsche Entomologische Zeitschrift, NF*, **39**, 295–367.

Krell, F.-T. (1996) Die Kopulationsorgane des Maikäfers *Melolontha melolontha* (Insecta: Coleoptera: Scarabaeidae) – Ein Beitrag zur vergleichenden und funktionellen Anatomie der ektodermalen Genitalien der Coleoptera. *Stuttgarter Beiträge zur Naturkunde (A)*, **357**, 1–101.

Krell, F.-T. (2000) The fossil record of Mesozoic and Tertiary Scarabaeoidea (Coleoptera, Polyphaga). *Invertebrate Taxonomy*, **14**, 871–905.

Kukalová-Peck, J. & Lawrence, J.F. (1993) Evolution of the hind wing in Coleoptera. *Canadian Entomologist*, **125**, 181–258.

Lacodaire, M.T. (1856) *Histoire Naturelle des Insectes. Genera des Coléoptères. Tome III. Pectinicornes et Lamellicornes*. Librairie Encyclopédique de Roret, Paris.

Lacroix, M. (2000) Hannetons, un monde de diversité. http://hannetons.free.fr (accessed June 2004).

Larsén, O. (1966) On the morphology and function of the locomotor organs of the Gyrinidae and other Coleoptera. *Opuscula Entomologica Supplementum*, **30**, 1–242.

Lumaret, J.P. & Tauzin, P. (1992) Le genre *Propomacrus* Newmann 1837, Données biologiques et morphologie larvaire. (Col. Scarab., Euchiridae). *Nouvelle Revue d'Entomologie (NS)*, **9**, 173–180.

Machatschke, J.W. (1959) Phylogenetische Untersuchungen über die Sericini (sensu Dalla Torre 1912) (Coleoptera: Lamellicornia: Melolonthidae). *Beiträge zur Entomologie*, **9**, 730–746.

Matsuda, R. (1965) Morphology and evolution of the insect head. *Memoirs of the American Entomological Institute*, **4**, 1–334.

Matsuda, R. (1970) Morphology and evolution of the insect thorax. *Memoirs of the Entomological Society of Canada*, **76**, 1–431.

McQuillan, P.B. (1985) The identification of root-feeding cockchafer larvae (Col. Scar.) found in pastures in Tasmania. *Australian Journal of Zoology*, **33**, 509–546.

Medvedev, S.I. (1952) *Lichinki Plastinchatousykh Zhukov Fauny SSSR. Opredeliteli po faune SSSR, izdavaemye Zoologicheskim. Institutom Akademii Nauk SSSR 47*. Akademia Nauk SSSR, Moskva/Leningrad.

Mikšić, R. (1976) *Monographie der Cetoniinae der Paläarktischen und Orientalischen Region*, Band 1. Šipad, Sarajevo.

Nel, A. & de Villiers, W.M. (1988) Mouthpart structure in adult scarab beetles. *Entomologica Generalis*, **13**, 95–114.

Nel, A. & Scholtz, C.H. (1990) Comparative morphology of the mouthparts of adult Scarabaeoidea. *Entomology Memoir, Department of Agricultural Development*, **80**, 1–84.

Nikolaev, G.V. (1998) Pleurostict Lamellicorn beetles (Coleoptera, Scarabaeidae) from Lower Cretaceous of Transbaikalia. *Palaeontological Journal*, **32** (77–84), 513–520.

Nixon, K.C. (1999) The parsimony ratchet, a new method for rapid parsimony analysis. *Cladistics*, **15**, 407–414.

Nixon, K.C. (2002) *Winclada (BETA)*, version 1.00.08. Published by the author, Ithaca.

Paulian, R. & Lumaret, J.P. (1982) Le larve des Orphnidae. (Col. Scarabaeoidea). *Bulletin de la Société Entomologique de France*, **87**, 263–272.

Pretorius, R., Philips, K. & Scholtz, C.H. (2000) Geometric morphometrics, the metendosternite and its use in phylogenetics of the Scarabaeinae (Coleoptera). *Elytron*, **14**, 125–148.

Ritcher, P.O. (1966) *White Grubs and their Allies. A Study of North American Scarabaeoid Larvae*. Oregon State Monographs. Studies in Entomology. Oregon State University Press, Corvallis.

Ritcher, P.O. (1969) Morphology of the posterior procoxal bridges in Scarabaeoidea. *Coleopterists Bulletin*, **23**, 89–92.

Sanmartín, I. & Martín-Piera, F. (2003) First phylogenetic analysis of the subfamily Pachydeminae (Coleoptera. Scarabaeoidea, Melolonthidae): the Palearctic Pachydeminae. *Journal of Zoological Systematics and Evolutionary Research*, **41**, 2–46.

Scholtz, C.H. (1990) Phylogenetic trends in the Scarabaeoidea. *Journal of Natural History*, **24**, 1027–1060.

Scholtz, C.H. & Browne, D.J. (1996) Polyphyly in the Geotrupidae (Coleoptera: Scarabaeoidea): a case for a new family. *Journal of Natural History*, **30**, 597–614.

Scholtz, C.H., Browne, D.J. & Kukalová-Peck, J. (1994) Glaresidae, archaeopteryx of the Scarabaeoidea. *Systematic Entomology*, **19**, 259–277.

Scholtz, C.H. & Chown, S.L. (1995) The evolution of habitat use and diet in the Scarabaeoidea: a phylogenetic approach. *Biology, Phylogeny, and Classification of Coleoptera: Papers Celebrating the 80th Birthday of Roy A. Crowson* (ed. by J. Pakaluk and S. A. Ślipiński), pp. 355–374. Muzeum i Instytut Zoologii PAN, Warszawa.

Simpson, G.G. (1980) *Splendid Isolation. The Curious History of South American Mammals*. Yale University Press, London.

Snodgrass, R.E. (1932) Evolution of the insect head and the organs of feeding. *Annual Report Smithsonian Institution*, **1931**, 443–489.

Snodgrass, R.E. (1935) *Principles of Insect Morphology*. Cornell University Press, Ithaca.

Strong, E.E. & Lipscomb, D. (1999) Character coding and inapplicable data. *Cladistics*, **15**, 363–371.

Takai, M., Anaya, F., Shigehara, N. & Setoguchi, T. (2000) New fossil material of the earliest new world monkey, *Branisella boliviana*, and the problem of platyrrhine origins. *American Journal of Physical Anthropology*, **111**, 263–281.

Tanner, V.M. (1927) The genitalia of female Coleoptera. *Transactions of the American Entomological Society*, **53**, 3–50.

Tashiro, H. (1987) *Turfgrass Insects of the United States and Canada*. Cornell University Press, Ithaca.

Williams, I.J. (1938) The comparative anatomy of the mouthparts of the order Coleoptera treated from the standpoint of phylogeny. *Journal of the New York Entomological Society*, **46**, 245–289.

Zunino, M. & Monteresino, F. (1990) Ideas preliminares sobre la evolucion de los aparatos copuladores en Rutelinae y la filogenia del grupo. *Revista de la Sociedad Entomologica Argentina*, **48**, 3–13.

Appendix 1. List of species studied for the cladistic analysis

The higher classification used here is based on Browne & Scholtz (1998, 1999). That of melolonthine lineages is partially based on Lacroix (2000) as well as Houston & Weir (1992). Species used as representatives for the genera in the analysis are marked with an asterisk

Trogidae

  Trox sabulosus (Linnaeus, 1758)*
  T. scaber (Linnaeus, 1767)
  T. unistriatus Palisot de Beauvois, 1818

Geotrupidae

  Anaplotrupes stercorosus (Scriba, 1791)

Scarabaeidae
Aphodiinae

  Aphodius hamatus Say, 1824
  A. pardalis LeConte, 1857
  A. scutator (Herbst, 1789)*
  A. rufipes (Linnaeus, 1758)

Scarabaeinae

  Copris lunaris (Linnaeus, 1758)*
  Onthophagus fracticornis (Preyssler, 1790)
  Catharsius molossus (Linnaeus, 1758)

Orphninae

  Orphnus sp.*
  Hybalus graecus Sturm, 1843

Euchirinae

  Propomacrus mucronatus (Pallas, 1781)*

Trichinae

  Trichius fasciatus (Linnaeus, 1758)*

Osmoderminae

  Osmoderma eremita (Scopoli, 1763)*

Cetoniinae

  Protaetia cuprea (Fabricius, 1775)*
  Tropinota hirta (Poda, 1761)
  Cetonia aurata (Linnaeus, 1761)

Valginae

  Valgus hemipterus (Linnaeus, 1758)*

Dynastinae

  Oryctes nasicornis (Linnaeus, 1758)*
  O. boas (Fabricius, 1775)
  Pentodon idiota (Herbst, 1789)
  Cyclocephala sp.

Rutelinae

  Adoretus sinicus Burmeister, 1855
  Adoretus sp.*
  Anisoplia (*Chaetopteroplia*) *segetum* Herbst, 1783*
  Anomala dubia (Scopoli, 1763)*
  Anomala spp.
  Anomala orientalis (Waterhouse, 1875)

Pachypodinae

  Pachypus candidae (Petagna, 1786)*

Melolonthinae
Melolonthini

  Amphimallon majale (Razoumowsky, 1789)
  A. solststiale (Linnaeus, 1758)*
  Macrophylla longicornis (Fabricius, 1787)*
  Melolontha melolontha (Linnaeus, 1758)*
  Pseudopanotrogus clypealis (Moser, 1915)
  Sparrmannia sp.

Pachydemini

  Elaphocera tangerina Kraatz, 1888*
  Elaphocera capdeboni Schauffuss, 1882
  Europteron gracile Marseul, 1867*

Hopliini

  Tanyproctus persicus (Ménétries, 1832)*

  Hoplia graminicola (Fabricius, 1792)*
  Hoplia equina LeConte, 1880

Chasmatopterini

  Chasmatopterus hirtus (Illiger, 1803)*

incertae sedis

  Acoma sp.*

Xylonichini

  Xylonichus eucalipti Boiduival, 1835*
  X. piliger Blanchard, 1851

Phyllotocini

  Phyllotocus macleayi Fischer von Waldheim, 1823*
  Anthotocus antennalis (Lea, 1919)

Diphucephalini

  Diphucephala spp.*

Scitalini

  Telura alta Britton, 1987*

Sericoidini

  Sericoides sp.*

Heteronycini

  Heteronyx sp.*

Ablaberini

  Camenta westermanni Harold, 1878*
  C. elongata Frey, 1960
  Cyrtocamenta pygidialis Frey, 1968*
  C. pygmaea Brenske, 1897
  Ablabera hirsuta Blanchard, 1850*
  Empecamenta buettikeri Ahrens, 2000*

Sericini

  Ablaberoides abyssinicus (Brenske, 1902)
  Amiserica chiangdaoensis Ahrens, 2003
  Astaena tridentata Erichson, 1847
  Astaena spp.*
  Athlia rustica Erichson, 1835*
  Calloserica langtangica Ahrens, 1999
  Comaserica bergrothi Brenske, 1900
  Gastroserica marginalis (Brenske, 1894)
  Hymenochelus distinctus (Uhagon, 1876)*
  Hymenoplia castilliana Reitter, 1890*
  Hyposerica spp.*
  Maladera castanea (Arrow, 1913)
  M. holosericea (Scopoli, 1772)*
  M. insanabilis (Brenske, 1894)
  M. simlana (Brenske, 1898)
  M. renardi (Ballion, 1870)
  Nepaloserica procera rufescens Frey, 1965
  N. schmidti Ahrens et Sabatinelli, 1996
  Omaloplia ruricola (Fabricius, 1775)*
  O. spireae (Pallas, 1773)
  Pachyserica olafi Ahrens, 2004
  Paratriodonta romana (Brenske, 1890)
  Pleophylla fasciatipennis Blanchard, 1850
  Pleophylla sp.*
  Raysymmela pallipes (Blanchard, 1850)*
  R. bruchi (Moser, 1924)
  Serica brunna (Linnaeus, 1758)*
  S. pommeranzi Ahrens, 1999
  Sericania fuscolineata Motschulsky, 1860
  Symmela instabilis Erichson, 1835*
  Triodontella raymondi Perris, 1869*
  T. dalmatica (Baraud, 1962)
  Trochalus sp.*

Appendix 2. Data matrix for the cladistic analysis. Inapplicable characters were coded as '–', whereas missing characters were coded as '?'. All characters were run as equally weighted and nonadditive. The Nexus file is available as supplementary material.

Character number	1 1234567890	1111111112 1234567890	2222222223 1234567890	3333333334 1234567890	4444444445 1234567890	5555555556 1234567890	6666666667 1234567890	7777777778 1234567890	8888888889 1234567890	9999999990 1234567890	1111111 0000000 1234567
Trox	000003320-	-000100000	0007101000	0011-00000	0?????0000	000-1002-1	2000000101	0001000002	000000---1	1000000000	-002000
Ablabera	1100021110	0100011101	1000100000	1101001000	0?????0000	0110010010	1100000102	1010001012	00101201-0	-21011-111	0112???
Ablaberoides	1100011010	0100110100	1110111110	1110-11100	0101111111	1111111010	1100010011	2000001020	0011121121	0200021111	1112???
Acoma	000103321-	--21000110	2000100010	1102000021	1?????0000	010-100000	4000000002	0010001010	000000-0-0	0000001???	???????
Adoretus	0000005011	-100111101	1000100000	1100000020	1101100000	0110010010	2301100001	0001011010	0100120111	2200001110	0011120
Amphimallon	0000041311	-001101101	1000100000	1102100021	1101100000	0110010010	4100000002	0001111110	12001200-0	0000001110	0011113
Anisoplia	0000001011	-100111101	1000100000	1100000020	1101100000	0110010010	2301100002	0001111110	020011-111	2200000110	0011120
Anomala	0000001011	-100111101	1000100000	1100000020	1101100000	0110010010	2301100002	0001111110	020011-111	2200000110	0111123
Anthotocus	000013321-	-100000110	0000101000	1102000110	0?????0000	0110010010	0000000002	1020001010	00000100-1	000001-???	???????
Aphodius	000003300-	-000100000	0000200000	0000001000	0010000000	000-010000	0000000001	0001012010	00000000-1	0000000110	0112024
Astaena	1100121010	0100100100	1001100000	1101001100	0?????0000	0110010000	1100000001	0000001010	0011121111	021011-111	1112???
Athlia	0000001011	-100011111	1000100000	1102002100	0?????0000	0110010010	0100000002	1020001010	00000200-0	0001-0-111	0112???
Camenta	1000021110	0100011101	1000101000	1010001000	0?????0000	0110010010	1200000101	1010001012	00101201-0	-20011-111	0112???
Chasmatopterus	000013321-	-210011101	1000101000	1101010020	0?????0000	0110010010	1100000002	2010011010	02000100-0	0000001110	0012???
Comaserica	1100011010	0100110110	0010111010	1110-11110	0101111111	1111110110	1100010011	2000001010	0011121121	1200121111	1112???
Copris	000003300-	-000100000	0000200020	0201001000	0010000002	000-010010	3000000001	1001012012	200000---1	1000000211	-112020
Cyrtocamenta	1100021110	0100011101	1000100000	1101001000	0?????0000	0110010010	1100000102	1010001012	00101201-0	-21011-111	0112???
Diphucephala	0000140011	-110000110	0001100000	1102001100	0?????0000	010-010210	3100000002	0000001010	00000200-0	0000000111	0111101
Elaphocera	000103321-	-100000110	2001100000	1102000021	0?????0000	010-000000	4100000002	0010011011	02000100-0	0000001110	0012???
Empecamenta	1100021110	0100011101	1000100000	1010001000	0?????0000	0110010010	1200000101	1010001012	00101201-0	-20011-111	0112???
Europteron	000103321-	--20000110	2000000000	2102000021	0?????0000	0110000000	4000000002	1010011011	020000-0-0	0000001110	0012???
Heteronyx	0000001011	0000100101	1000101000	1101001000	0?????0000	0110110010	0100000002	0000001010	00000100-0	000001-111	0111102
Hoplia	0000022010	-100000110	0001100000	1102000120	1?????0110	210-011010	-001100002	1002001010	200000-0-0	0000000110	0012100
Hymenochelus	1100011010	1100111111	1000111010	1110-11110	0101110110	1110010110	1110010001	2000001010	0011121101	011001-111	1112???
Hymenoplia	1100021010	1100011111	1000111010	1110-11110	0101110110	1110010110	1110010001	2000001010	0011121101	011001-111	1112???
Hyposerica	1100011010	0100110100	0011111010	1110-11110	0101111111	1111110010	1100010011	2000001010	0011121121	1200121111	1112???
Macrophylla	000003131-	-001001100	1000100000	1102100021	1?????0000	010-010010	4100000002	1001111110	00000200-0	0000000???	???????
Maladera	1100011010	0100110100	1111111110	1110-11110	0101111110	1111010010	1100010011	2000001020	0011121??1	1100121111	1110101
Melolontha	0000041311	-001101101	1000100000	1102100021	1101100000	0110010010	4100000002	0001111110	12001200-0	0000000110	0011123
Omaloplia	1100011010	0110100100	0010111010	1110-01110	0101111111	1111011010	1100010011	2000001010	0011121??1	1210021111	1110101
Orphnus	000003400-	-000000000	0000200000	1102001000	0?????0000	0110110010	1000000000	0001011010	000000-111	2000000100	0010101

Taxon										
Oryctes	000003321–	1000100000	2102000021	1101100000	0110110011	2000000001	0001111110	0100020110	2000000110	0012120
Osmoderma	001003321–	0001100001	2102010021	1??????00100	010–010011	2000001002	1101111110	010000–100	2000001110	0011220
Pachypus	100113321–	––21000110	2112–00001	0??????0000	010–100000	1000000002	1010011011	000000–0–0	0000001110	0012????
Phyllotocus	010013321–	–100100000	1102000100	0??????10100	0110010010	0000000002	0010010010	0000000200–0	0000011010	0110100
Pleophylla	1100011011	0110111101	1110–11110	0??????1111	1111010110	1100010011	2000010010	0011121??1	1210021111	111?????
Protaetia	001003321–	–100111101	1001010021	1101100001	010–010011	2000001002	–101111102	0200010100	2001001110	0011220
Propomacrus	000003321–	–100011101	2102000021	1??????0000	010–010011	2100000002	1001011110	000000–0–0	0000000111	0012110
Raysymmela	1100121010	0100100100	1101101100	0??????10000	0110010110	1100000001	0000001010	0011121111	0210121111	111?????
Serica	1100011010	0100110100	1110–11110	0101111111	1111010010	1100010011	0000001020	0011121101	1100121111	1110101
Sericoide	0000000011	–100000101	1101001100	0??????00000	0110110010	0000000002	0000001010	0000010000	000001–111	011?????
Synmela	1100021010	0100100100	1101001100	0??????10000	0110010110	1100000001	0000001010	0211121111	0210121111	111?????
Tanyproctus	000003301–	–000001101	1000100000	0??????00000	0110010010	4100000002	0010011011	0200100–0	0000001110	0010112
Telura	0001140011	–100111101	1000100000	1101100100	0110010010	0000000002	0000001010	0000000100–0	0000011111	0110101
Trichius	000003321–	–100111111	1002010021	1101100100	010–010010	2000000002	0001111100	0200010100	2000001110	0011220
Triodontella	1100021010	0100011111	1010111010	0??????10110	1111010110	1100010011	2000001010	0011121101	0110021111	1110100
Trochalus	1100011011	0100110100	1110–01110	0??????11111	1111011110	1100010011	2000001020	0011121121	0200121111	111?????
Valgus	001003321–	–100111111	1100000021	1101100001	010–010010	2000001002	1101111102	220010–100	2010000110	0011220
Xylonichus	0000041311	–000000101	1102000021	1??????00000	0110010010	0000000002	0020001210	0200100–0	0000011111	011????

Appendix 3. Abbreviations used in the figures

A	anal anterior (anal vein)
abstn	abdominal sternite
abt	abdominal tergite
ah	apical hinge of wing
almf	anterior lamina of mesofurcal arm
amlc	anterior margin of labroclypeus
ammtf	anterior margin of metafurca
anl	anal lobe (elytral base)
anspl	anal split
ant	antenna
aph	anterior phragma
apmtf	anterior portion of metafurca
apophb	apodeme of phallobase
apvfl	apical portion of ventral median flange
ax2	axillary 2
ax3	axillary 3
bg	basigalea
bma	anterior part of medial basivenale
bophb	basal ostium of phallobase
bsc	subcostal basivenale
bst	basistipes
bucop	bursa copulatrix
c	coxite
cd	cardo
clv	clavus
cly	clypeus
crspic	cranial part of spiculum gastrale
CuA	cubital vein
cxo	coxal ostium
dg	distogalea
dLmf	dorsal lamina of mesofurcal arm
dmmttb	dorsal margin of metatibia
dmtbs	dorsal apical metatibial spur
dpmst	dorsal process of mediostipes
dstgl	distal separate tooth of galea
el	elytron
enpl	(pro-)endopleuron
eph	endophallus
eppl	epipleuron
esh	elytral shelf
expl	(pro)exopleuron
fm1	median plate, part 1
fm2	median plate, part 2
fr	radial fulcalare
frcs	frontoclypeal suture
frs	frons
gl	galea
glacc	accessory gland
glrec	glandula receptaculi
hp	humeral plate
hpmr	haptomerum
hymr	hypomeron
ifb	interfurcal bridge
ifl	internal flange of longitudinal suture of metasternum
iowth	interocular width
lbr	labrum
lbrcly	labroclypeus
lc	lacinia
li	ligula
ll	ligular lobe

mamtco	medial apophysis of metacoxa
mepstm	metepisternum
msco	mesocoxa
mscoc	mesocoxal cavity
msfa	mesofurcal arm
msfe	mesofemur
msstm	mesosternum
mst	mediostipes
mstb	mesotibia
mstrm	mesotarsomere
mt	mentum
mtco	metacoxa
mtepst	metepistenum
mtf	metafurca
mtfa	metafurcal arms
mtfe	metafemur
mtn	metanotum
mtstm	metasternum
mttb	metatibia
mttrm	metatarsomere
octs	ocular canthus
ovd	common oviduct
p	proctiger
p1	dorsal process of mesofurcal arm
p2	cranial process of mesofurcal arm
p3	medial process of mesofurcal arm
pal	palidium
pf	palpifer
pg	palpiger
phb	phallobase
pl	palpus labialis
pm	parameres
pmmtf	posterior margin of metafurca
pmx	maxillary palpus (palpus maxillaris)
pon	postnotum
pp	paraproct
prmt	prementum
prn	pronotum
prpyg	propygidium
prtb	protibia
pyg	pygidium (urotergite VIII)
RA	radius anterior
rms	radio-medial suture
RP	radius posterior
rs	receptaculum seminis
scl	scutellum
somtco	secondary ostium of metacoxa
sty	stylus
te	temones
tlsgl	toothlike spines of galea
tr	trochanter
trc	transversal carina of procoxa
vag	vagina
vfl	ventral median flange
vf	valvifer
vmmttb	ventral margin of metatibia
vmtbs	ventral apical metatibial spur
vpphb	ventral plate of phallobase
vs	ventral suture (of metendosternite)
vsp	'v-shaped' piece
vst	vestigial sternite